

ELUCIDATING THE ROLE OF CELL TO EXTRACELLULAR MATRIX ADHESION IN
REGULATING TISSUE MECHANICS DURING DEVELOPMENT

by

KATHARINE ELIZABETH GOODWIN

B.Sc., University of Toronto, 2013

A THESIS SUBMITTED IN PARTIAL FULFILLMENT OF
THE REQUIREMENTS FOR THE DEGREE OF

MASTER OF SCIENCE

in

THE FACULTY OF GRADUATE AND POSTDOCTORAL STUDIES

(Cell and Developmental Biology)

THE UNIVERSITY OF BRITISH COLUMBIA

(Vancouver)

November 2015

© Katharine Elizabeth Goodwin, 2015

Abstract

Tissue morphogenesis requires force-generating mechanisms to drive the organization of cells into complex three-dimensional structures. Although such mechanisms have been characterized across the metazoan lineage, we know little about how force transmission across a tissue is regulated. Here, using *Drosophila melanogaster* as a model system, I provide evidence that integrin-mediated cell-ECM adhesion is required for the regulation and transmission of forces in tissues. Specifically I show that during Dorsal Closure (DC), an integrin-dependent morphogenetic process that occurs during *Drosophila* embryogenesis, failure to regulate the level of cell-ECM adhesion results in abnormal levels of tension in the amnioserosa (AS), an extra-embryonic epithelium that is essential for DC. Integrin-containing adhesive structures were identified on the basal surface of the AS that share many features with focal adhesions. Using mutations that either increase or decrease integrin-based Cell-ECM adhesion, I show that DC is defective in both cases, and that the level of adhesion is inversely correlated with the mobility of cells in the AS. Mathematical modeling, quantitative image analysis, and in vivo laser ablation experiments reveal a relationship between cell mobility and the magnitude, distribution and transmission of tension in the AS. Finally, I provide evidence that mechanical coupling exists between AS cells and their substrate, the underlying ECM and the yolk membrane. Overall, my data shows that integrins regulate the transmission of forces across the AS, and thereby control a critical component of DC. I propose that modulating Cell-ECM adhesion could provide control over force transmission within developing tissues to promote specific outcomes.

Preface

A version of this work is in revisions for publication. Guy Tanentzapf and I conceived experiments and designed the project with support and ideas from Emily Lostchuck and Stephanie Ellis. Emily Lostchuck, Stephanie Ellis, Daniela Gunne and Steven Meng assisted with a subset of fly genetics, sample preparation and image acquisition. Steven Meng, Walter Wasserman and I performed all computational analysis. The mathematical model used in this work was created by James Feng (University of British Columbia), who also assisted me in applying it to our research. Teresa Zulueta-Coarasa and Rodrigo Fernandez-Gonzalez (University of Toronto), assisted me with laser ablation experiments.

Table of Contents

Abstract.....	ii
Preface.....	iii
Table of Contents.....	iv
List of Figures.....	vi
List of Abbreviations.....	vii
Acknowledgements.....	viii
Chapter 1: Introduction.....	1
1.1. Mechanical forces during <i>Drosophila</i> morphogenesis.....	1
1.1.1. Dorsal closure.....	4
1.1.2. Mathematical models of DC.....	6
1.2. Mechanical forces in cell culture models.....	9
1.2.1. Single cell migration.....	11
1.2.2. Collective migration and cell clusters.....	13
1.3. Morphogenesis and cell adhesion.....	14
1.3.1. The integrin adhesion complex.....	14
1.3.2. Integrin-mediated adhesion in cell culture.....	16
1.3.3. Integrin-mediated adhesion in <i>Drosophila</i> embryogenesis.....	18
1.3.4. Integrin-mediated adhesion in embryogenesis of other model organisms.....	20
1.4. Aim and scope of thesis.....	21
Chapter 2: Materials and methods.....	23
2.1. Fly stocks and genetics.....	23
2.2. Live imaging.....	24
2.3. Laser ablation.....	25
2.4. Image analysis.....	25
2.4.1. Closure rate, AS shape and cell extrusion.....	25
2.4.2. FALS morphology and tracking.....	25
2.4.3. Cell morphology and movement.....	26
2.4.4. MSD analysis.....	28
2.4.5. Cell movement correlation.....	28
2.4.6. Nucleus tracking.....	28

2.4.7. Recoil after laser ablation	29
2.4.8. Cell-substrate movement correlations.....	30
2.5. Mathematical model of DC	32
Chapter 3: Results	33
3.1. Focal adhesion-like structures in the AS.....	33
3.2. Cell-ECM adhesion is required for DC.....	35
3.3. AS cell mobility is modulated by cell-ECM adhesion.....	37
3.4. Global patterns of cell movement and tension in the AS.....	40
3.5. Cell-ECM adhesion regulates global AS cell movement and tissue tension	43
3.6. Force-generation and tissue biomechanical properties in the background of altered cell-ECM adhesion	45
3.7. Cell-ECM adhesion controls force transmission in the AS.....	48
3.8. Cell-cell and cell-substrate movement correlations in the AS	51
Chapter 4: Discussion	57
4.1. Overview of findings.....	57
4.2. Limitations and proposed future work	61
4.2.1. Potential confounding factors	61
4.2.2. Apical vs basal cell dynamics	63
4.2.3. Mathematical model of DC.....	65
4.2.4. Cell-substrate interactions.....	66
4.3. Conclusion.....	68
References.....	70

List of Figures

Figure 1.1. Cell area ratcheting <i>in vivo</i> and <i>in silico</i>	3
Figure 1.2. <i>Drosophila</i> germband retraction and dorsal closure.....	5
Figure 1.3. Mechanical forces in cell culture models.....	10
Figure 2.1. Automatic segmentation of FALS in the AS.....	27
Figure 3.1. FALS are dynamic, mechanosensitive adhesion sites in the AS.....	34
Figure 3.2. Modulating cell-ECM adhesion affects FALS morphology.....	35
Figure 3.3. Cell-ECM adhesion is required for DC.....	36
Figure 3.4. AS cell mobility is modulated by cell-ECM adhesion.....	38
Figure 3.5. A mathematical model of DC suggests a role for friction in cell movement and closure phenotypes.....	39
Figure 3.6. Global patterns of cell movement and tension in the AS.....	41
Figure 3.7. Spatiotemporal differences in cell-ECM adhesion and cell movement in the AS.....	43
Figure 3.8. Cell-ECM adhesion regulates movement patterns and tension in the AS.....	44
Figure 3.9. Cell-ECM adhesion controls AS cell area oscillations.....	46
Figure 3.10. Tissue mechanical properties in embryos with altered cell-ECM adhesion.....	47
Figure 3.11. Cell-ECM adhesion controls force transmission in the AS.....	50
Figure 3.12. Decreased cell-ECM adhesion results in more transmission of cell movement.....	52
Figure 3.13. AS cell movement correlates with in-plane substrate displacements.....	54
Figure 3.14. Fluctuations in AS cell area are accompanied by changes in substrate height.....	56
Figure 4.1. Proposed model of cell-ECM adhesion-mediated force transmission in the AS.....	69

List of Abbreviations

AJ	adherens junction
AP	anterior-posterior
AS	amnioserosa
Bsg	Basigin
CA	constitutively active
DC	dorsal closure
DV	dorsal-ventral
ECM	extracellular matrix
FA	focal adhesion
FALS	focal adhesion-like structures
GBR	germband retraction
GFP	green fluorescent protein
GTP	Guanine triphosphate
IAC	integrin adhesion complex
IBS-1	integrin binding site 1
IBS-2	integrin binding site 2
ML	medial-lateral
MSD	mean squared displacement
<i>mys</i>	<i>myspheroid</i>
NA	numerical aperture
nbr	neighbour
PIV	particle image velocimetry
RFP	red fluorescent protein
RIAM	Rap1-GTP-interacting adapter molecule
TFM	traction force microscopy
WT	wild-type

Acknowledgements

I would like to extend my gratitude to the many people who have helped me throughout my graduate studies. Firstly, I would like to thank my supervisor, Guy Tanentzapf, for his guidance and support. I have learned a great deal about how to perform and especially communicate scientific research from him. I would also like to thank Tanentzapf lab members past and present. In particular, Emily Lostchuck and Stephanie Ellis contributed a great deal to the work presented in this thesis. Emily provided invaluable support every step of the way, especially with genetics (my favourite), and Stephanie planted the seeds for this project before leaving to begin postdoctoral work, and has continued to help with manuscript writing. I would also like to thank a few undergraduate students who made significant contributions. Daniela Gunne was a fantastic undergraduate thesis student who helped me to develop a quantitative image analysis pipeline. Steven Meng (The Oracle) and Walter Wasserman very quickly became master MatLab-ers working with me, and have helped me figure out my own analysis problems while also independently developing tools (and fixing every piece of electronic equipment in the lab). I would also like to thank the remaining members of the lab, Amanda Haage, Pablo Lopez-Ceballos, Michael Fairchild, Christopher Smendziuk, Fayeza Islam, Darius Camp and Rohan Khadilkar for their scientific help and advice, and for their friendship.

The work in this thesis was made possible thanks to our two collaborators, Jimmy Feng and Rodrigo Fernandez-Gonzalez, and the members of their labs. Jimmy and Rodrigo made it possible for us to conduct advanced biophysical analyses, and were always quick to give invaluable feedback on my manuscript and talks. Additionally, I would like to thank my committee members, Dan Coombs and Kurt Haas for their critiques and suggestions on my committee meetings and talks throughout my graduate work. I am also grateful for the support and advice from many other professors and students in the LSI, in particular Doug, John, Cal and Anthony.

Finally I would like to thank friends and family: LG, BG, MG, FM, SB, JA and JJ.

Chapter 1: Introduction

Animal development requires the rearrangement and remodelling of cells and tissues in order to generate a complex body plan, a process known as morphogenesis¹⁻³. During embryogenesis, stereotypic patterns of morphogens and gene expression direct the specification, proliferation, and relocation of cells, leading to tissue rearrangements. These morphological changes generate mechanical forces which can further influence cell behaviour, as well as regulate expression of developmental genes¹. Throughout development, cells respond to and exert intra- and intercellular forces upon their neighbours and surrounding environment. Structural changes and force generation in cells are achieved by the interactions between the actin cytoskeleton and two types of cellular adhesions; those connecting to adjacent cells and those anchoring cells to the extracellular matrix (ECM)^{2,4}. Both development and tissue homeostasis rely on cell and tissue mechanics. Failure to regulate cell structure and adhesion can arrest development in embryonic stages, and in adults such disruption can result in defective wound healing, as well as cancer and metastasis⁴⁻⁶. In order to understand how cell mechanics contribute to the formation and homeostasis of organisms, it is necessary to determine the relationships between cell behaviour, adhesion and biophysical forces throughout development.

1.1. Mechanical forces during *Drosophila* morphogenesis

Many studies of force-generating mechanisms during development have been performed in *Drosophila melanogaster*, a genetically tractable model organism. The various steps resulting in animal development, such as axis elongation and mesoderm invagination, are highly conserved across species, including *Drosophila*. Furthermore, technological advances in microscopy and fluorescent transgenes over the last decades have facilitated live-imaging of fly morphogenesis,

making it an excellent system in which to study cell and tissue level behaviours during development.

Forces that drive morphogenetic movements are derived from a number of sources including coordinated cell proliferation⁷, junctional remodelling^{8,9}, and cell shape changes^{10,11}. An example of how coordinated cell proliferation is used to generate force occurs in *Drosophila* wing disc morphogenesis, during which certain populations of cells proliferate at different rates, generating different levels of tension across the epithelium⁷. Subsequently, the resulting global pattern of mechanical force induces directional cell proliferation and cell shape changes in order to achieve a prescribed tissue shape⁷. The wing disc is an example of how tissue-wide forces can affect changes in cell morphology and behaviour, but there are also many situations in which cell behaviour is the source of tissue shape changes. An example of junctional remodelling as a force for morphogenesis occurs during axis elongation in *Drosophila*; cell-cell adhesion sites called adherens junctions (AJs) in the germband undergo myosin dependent remodelling within the apical plane, effectively shortening medial-lateral (ML) junctions and extending anterior-posterior (AP) junctions to allow cells to move in between their neighbours in a process called intercalation⁸. Coordinated intercalation of cells towards the midline results in ML contraction and AP extension of the germband⁸. Junctional remodelling also occurs along the apical-basal axis of cells, as in epithelial folding during *Drosophila* gastrulation⁹. In cells which initiate folding, AJs shift basally while remaining stationary in adjacent cells, facilitating tissue shape change⁹. Cell shape changes are also critical in epithelial folding, when cells constrict apically in order to change tissue topography^{10,11}. During apical constriction, medial actomyosin networks induce cycles of contraction and relaxation of cell area, behaving as a ratchet to stabilize cells at a smaller area at each step (Fig. 1.1. A and ¹¹). A similar ratchet mechanism has been observed in the context of

dorsal closure (DC, discussed in detail below), in which cell contraction is driven by actomyosin networks gradually reducing the apical area of oscillating cells in order to reduce the area of an entire tissue¹². However in the case of DC, there are many alternative and redundant mechanisms which play roles of varying importance at different stages of closure.

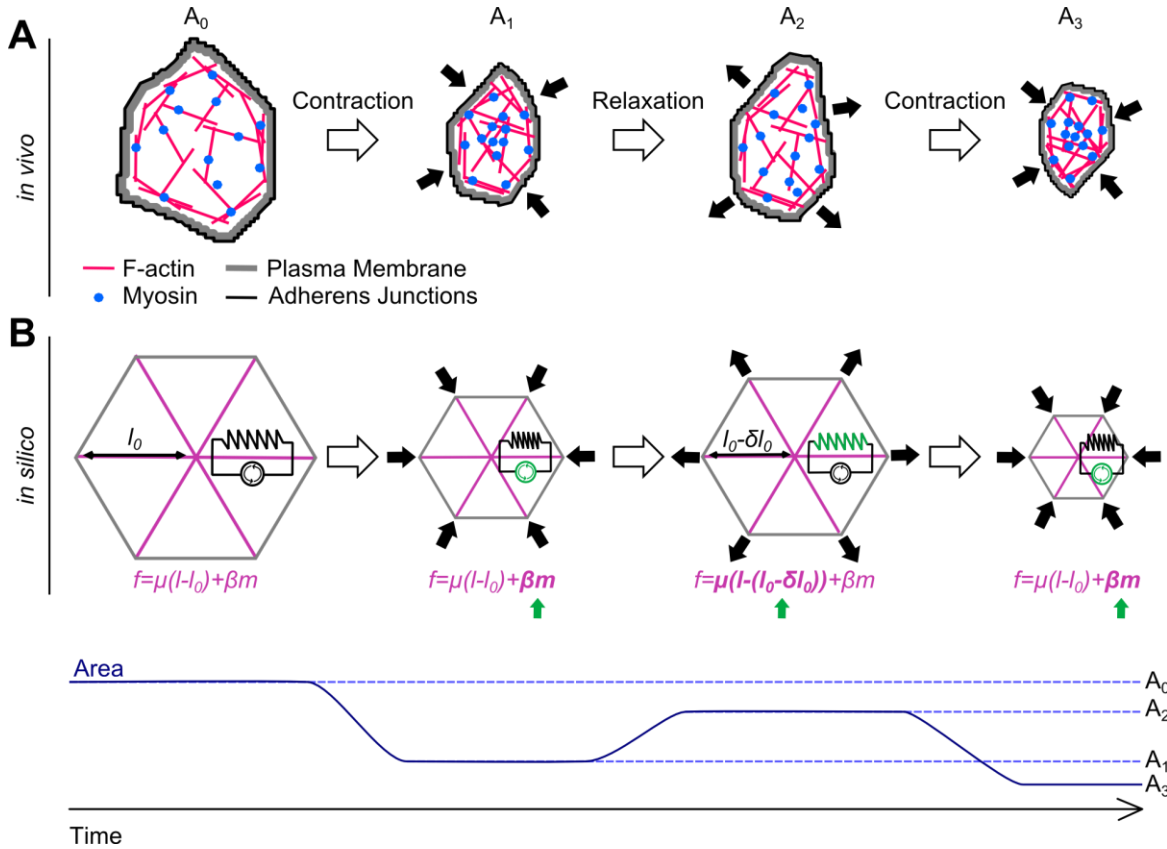


Figure 1.1. Cell area ratcheting *in vivo* and *in silico*

(A) Top view schematic of a cell *in vivo* undergoing ratcheting adapted from Martin et al, 2009¹¹. Myosin (blue) drives the contraction of an actin network (pink) coupled to adherens junctions (black) in order to decrease cell area from A_0 to A_1 . As the network relaxes, cell area will increase to a lower, stabilized area A_2 due to accumulation of junctional actomyosin, before contracting again to a smaller area, A_3 . (B) Schematic of a cell *in silico* adapted from Wang et al, 2012 and Machado et al, 2014^{13,14}. Spokes (purple) are subject to active contractile forces ($\beta m - \beta$ is the tensile force per myosin motor, m is the number of myosin motors) and passive elastic forces ($\mu(l - l_0) - \mu$ is the elastic modulus, $(l - l_0)$ is the deviation from rest length l_0). When contractile forces on the spokes increase (green), cell area contracts from A_0 to A_1 . Elastic resistance (green) to contraction then causes cell area to relax, and by incrementally decreasing the rest length by δl_0 , cells will stabilize at a smaller maximum area, A_2 , before contracting again to A_3 . Plot at the bottom shows cell area at each step.

1.1.1. Dorsal closure

DC involves the migration and fusion of two epithelial sheets over an extra-embryonic tissue, the amnioserosa (AS), in order to form a smooth epithelium on the dorsal side of the embryo¹⁵⁻¹⁷ (Fig. 1.2. B-D'). The forces involved in DC can be divided into 3 types: contractile forces generated by the AS, resistance of the surrounding epithelia, and tension in a supracellular purse-string surrounding the dorsal hole (Fig. 1.2. B'). Contractile forces within the AS are generated through multiple mechanisms. Pulses of medial actomyosin networks induce AS cell area oscillations, and promote apical constriction in order to drive tissue contraction^{12,18}. Tissue area is also globally decreased through cell extrusion, which has been proposed as an “apoptotic force” during DC¹⁹. More recently, a caspase-dependent, gradual volume loss in AS cells has been shown to cause AS contraction, independently of complete cell extrusion from the tissue layer²⁰. Furthermore, it was shown that internal pressure in the AS opposes contraction, and that volume loss may serve to counteract this force²⁰. The many contractile forces in the AS (represented as F_{AS} in Fig. 1.2. B') are opposed by a resistance to movement of the epidermis ($F_{epidermis}$) and aided by tension in generated in the leading edge ($T_{actin\ cable}$). This tension is generated by a supracellular actin cable or purse-string which forms around the dorsal hole^{15,21,22}. For closure to proceed, contractile forces in the AS and tension in the actomyosin purse-string must overcome $F_{epidermis}$ in order to pull the epidermis dorsally. In the late stages of closure and beginning at the canthi (anterior and posterior ends of the dorsal hole, Fig. 1.2. C'), actin-rich protrusions from the leading edge of the advancing epithelia meet and interdigitate in order to form a seam and close the dorsal hole (Fig. 1.2. D')^{23,24}.

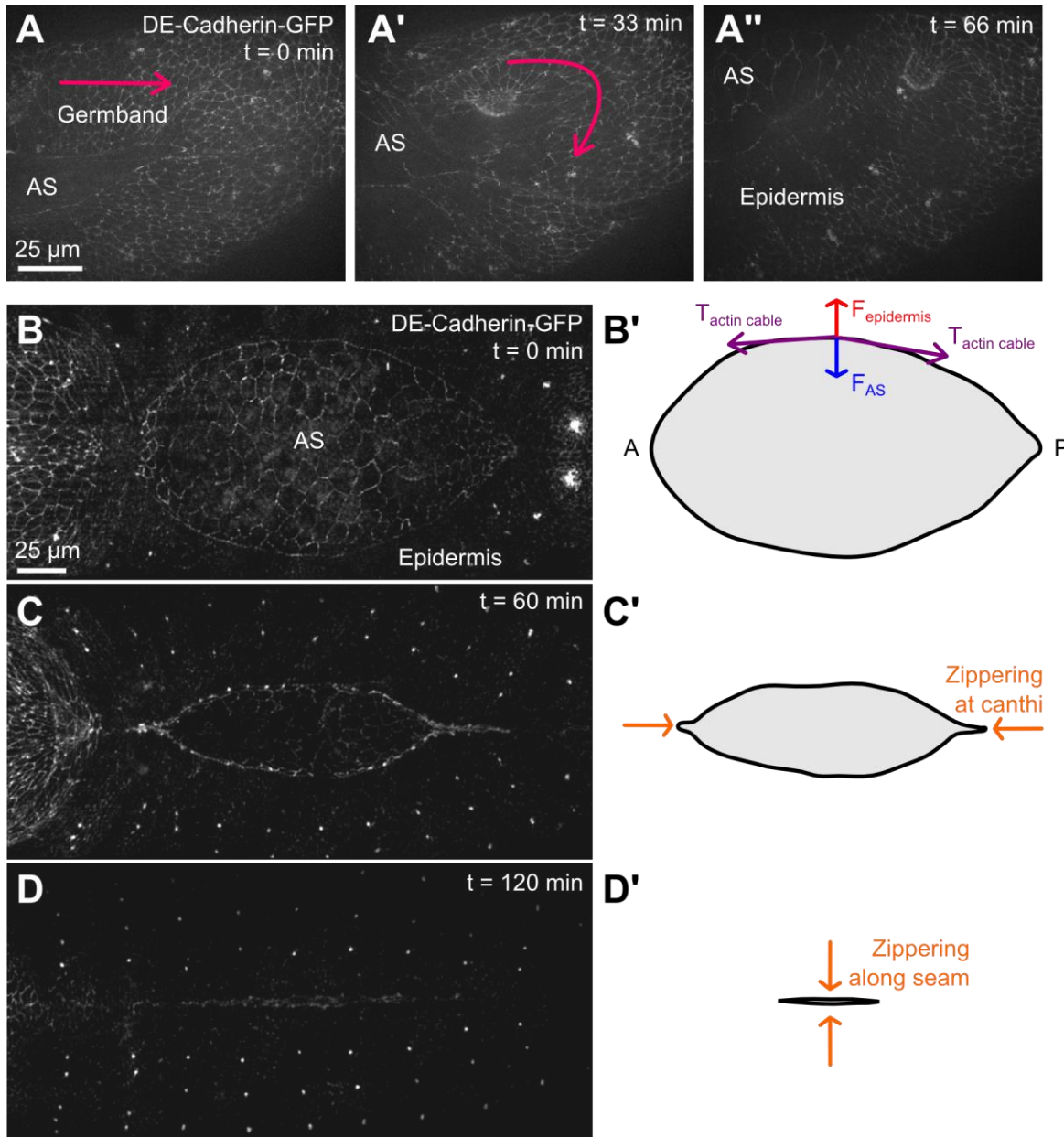


Figure 1.2. *Drosophila* germband retraction and dorsal closure

(A-A'') Images of embryo expressing DE-Cadherin-GFP undergoing germband retraction. AS, germband and epidermis indicated. Arrows indicate direction of germband movement. (B-D) Images of embryo expressing DE-Cadherin-GFP undergoing DC. Amnioserosa (AS) and epidermis are indicated. (B') Outline of AS with schematic force diagram for a given point along the edge of the AS. Force generated by the AS is indicated in red, resistive force of epidermis in blue, and tension generated in supracellular actin cable in the leading edge of the epidermis in purple. (C') Zippering at canthi indicated by orange arrows. (D') Zippering along the length of the seam brings surrounding epidermis into direct apposition and seals the hole to end DC.

While both contractile forces generated by the AS and by the surrounding epithelia contribute to closure, there has been some disagreement as to which plays a more important role. One model, favouring the surrounding epithelium, suggests that ratcheting and overall constriction of AS cells are achieved by the actomyosin cable in the leading edge. As cells oscillate in apical area, the advancing leading edge would theoretically restrict the amount of area relaxation, resulting in net tissue constriction. This is supported by the observation that oscillations become damped in cells closer to the leading edge before those towards the middle of the AS²². However, inhibiting actin cable formation in leading edge cells does not affect oscillation and constriction of AS cell area, favouring a cell-autonomous, ratcheting model of AS contraction¹². Further, laser microsurgery in live embryos revealed that complete removal of both canthi during DC did not prevent closure from completing at a near normal rate, despite completely abrogating purse string curvature and tension, and inhibiting zippering at canthi²⁵. Laser dissection of the AS to prevent AS-generated contractile forces also did not prevent closure, but resulted in greatly increased DC completion time¹⁵. Taken together, these studies show that contractile forces generated in the AS are sufficient but not necessary for DC.

1.1.2. Mathematical models of DC

Various mathematical models of DC have been developed in order to understand the role and relative importance of the multiple force generating mechanisms contributing to closure. Hutson et al. developed one of the first models of DC, in which the balance of forces generated by the AS, the epidermis, and tension in the purse string (Fig. 1.2. B') was used to predict how AS height would evolve over time¹⁵. They also included the effects of zippering, and concluded that the early phases of the DC were primarily driven by the AS, while zippering was critical in the late stages of closure. Further models have been developed to explore the role of zippering^{26,27} but as

the focus of this thesis is on the role of the AS, I will focus on models which explored the dynamics of AS cells during closure.

As the importance of forces generated by the AS became apparent from experimental data, attention focused to understanding possible force generation mechanisms, and in particular, the role of AS cell dynamics during tissue contraction. The model developed by Solon et al. was based on their observation that AS cells oscillate in apical area, and that these oscillations become damped over time – they therefore included the dynamics of individual AS cells in order to predict how they might contribute to DC²². The AS was represented by an array of polygons in which the spokes connecting each vertex and the center of mass were represented by viscoelastic elements subject to an applied contraction force to drive oscillation²². They also sought to uncover the contributions of the supracellular actin cable in the leading edge, represented as an elastic surrounding the AS and fixed at both ends²². The model replicated cell oscillations and contraction, and by increasing tension in the actin cable, was able to predict the initiation of closure; however, cell pulses stopped shortly after tissue contraction due to a loss of tissue tension²². Based on their experimental observations, they resolved this issue by forcing cells on the periphery to contract earlier than cells in the center, allowing pulsatile behaviour and therefore tension to persist in the middle of the AS²². While introducing a spatial gradient of pulsation arrest allowed the model to proceed normally, it raises the question of what biological mechanisms would cause different patterns of cell oscillations – it could be due to the influence of the actin cable under tension, as they suggest, or to unknown signalling pathways. Furthermore, it does not rule out the possibility that other mechanisms might contribute to persistent tension in the AS, such as the increase in junctional and medial myosin recruitment observed by Blanchard et al¹².

In order to better understand the molecular basis of driving forces generated in the AS, further models were developed which included the dynamics of actin and myosin. Two examples of this type of model were developed separately by Wang et al.¹³ and Machado et al.¹⁴. The representation of AS cells was similar to that described by Solon et al. - both models connect cell centers and vertices with spokes subject to passive viscoelastic forces (Fig. 1.1.B)^{13,14,22}. However, they each applied contractile forces in different manners – the Wang et al. model used attachment and detachment of myosin motors mediated by a putative signaling molecule¹³, and the Machado et al. model used actin turnover-dependent myosin contractile forces¹⁴. In each case, cell oscillations were effectively reproduced, and using outside modifications to the system (a gradual decrease of resting spoke length, Fig. 1.1. B), cell and tissue contraction was also achieved^{13,14}. While these models provide insight into the mechanisms by which actomyosin networks control cell oscillations, the question of what biological signals actually cause changes in pulsatile actomyosin network and cell contraction remains unanswered.

There is growing evidence suggesting that feedback loops between the polarity proteins of the Partitioning defective (Par) complex, specifically Par-6, atypical protein kinase C (aPKC) and Par3/Bazooka (Baz), may regulate actomyosin activity during DC²⁸. Actomyosin networks recruit the Par-6-aPKC complex to the apical domain of AS cells, where it downregulates actomyosin networks²⁸. Subsequently, aPKC recruits Baz to the apical domain, where Baz inhibits aPKC and thus favours actomyosin networks. These negative feedback loops allow for pulsatile actomyosin behaviour in which Baz stabilizes actomyosin networks and aPKC inhibits their formation²⁸. As closure proceeds, Baz-aPKC interactions increase, allowing actomyosin networks to transition from pulsatile to persistent – a necessary step for ratcheting and contraction of AS cell area. These findings were validated by adapting the Wang et al. model described above²⁸. In order to determine

the effect of decreasing inhibition of myosin networks, they reduced two rate constants associated with inhibiting the addition of myosin motors to spokes²⁸. The resulting simulations showed that cell pulses were quickly dampened, providing support for the control of actomyosin networks via negative feedback loops proposed by the authors²⁸.

Another important conclusion drawn in both studies was that a cell-autonomous, internal ratcheting mechanism was the main driving force behind tissue contraction during DC, instead of an external, supracellular actin cable driven ratchet, as proposed by Solon et al^{13,22}. This was only directly tested in the Wang et al. model – they determined that external ratcheting in the absence of internal ratcheting impaired tissue contraction, in disagreement with the model proposed by Solon et al^{13,22}. Each of these different mathematical models (Solon, Wang and Machado) have each been used to illustrate and support either cell-autonomous or leading-edge driven contraction theories; while their design and conclusions differ, they allow us to test our predictions about force-generating mechanisms during DC. Overall, simulations of DC are limited by their necessary simplifying assumptions, but they are nevertheless a valuable tool with which to gain insight into the driving forces behind morphogenetic movements.

1.2. Mechanical forces in cell culture models

A good deal of our understanding of how cells interact mechanically with each other and with their environments comes from studies of cells in culture. Since their physical surroundings can be controlled and engineered, it is possible to tease apart and even precisely measure the various forces exerted by cells. Using these tools, investigators have well characterized the events involved in single cell and collective migration, as well as the behaviour of clusters of stationary cells. Cell migration events are present throughout the development of an organism, as well as during adult life (e.g. immune cell migration) and diseases (e.g. invasive and metastatic cancers).

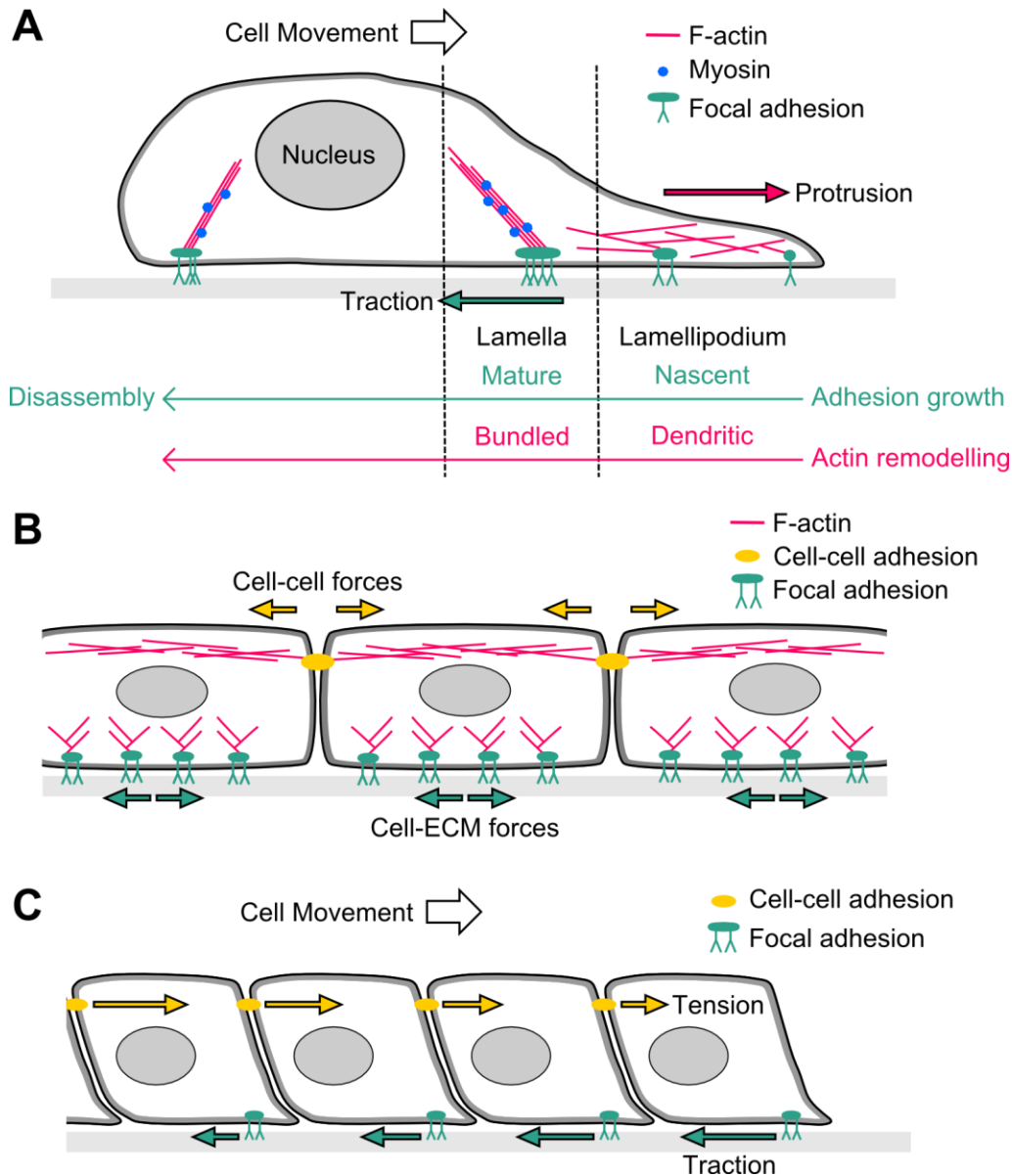


Figure 1.3. Mechanical forces in cell culture models

(A) Schematic of single cell migration *in vitro* adapted from Schwarz and Gardel, 2012²⁹. At the leading edge of the cell (lamellipodium), dendritic actin networks (pink) drive cell protrusion and nascent adhesions (teal) form and generate traction. As the cell advances, actin networks are remodelled into bundles and adhesions mature into FAs in a myosin (blue) dependent manner. At the rear of the cell, FAs are disassembled. (B) Schematic of epithelial clusters *in vitro* adapted from Ng et al, 2014³⁰. Cells adhere to the substrate via FAs (teal) and to each other via cell-cell adhesions (yellow). Both adhesive sites are associated with actin networks (pink), and participate in cell-ECM and cell-cell forces, respectively. (C) Schematic of the tug-of-war model for *in vitro* collective migration adapted from Trepant, 2012³¹. Each cell generates traction (teal arrows), which is partially transmitted to the cells following it, resulting in increasing tension (yellow arrows) with increasing distance from the leading edge, transmitted via cell-cell junctions.

1.2.1. Single cell migration

During single cell migration (Fig. 1.3. A), networks of actin cause the cell membrane to protrude in the direction of motion, generating a structure known as the lamellipodium^{29,32}. Nascent integrin-based adhesions (discussed in 1.3.2) form at the leading edge, and subsequently mature and recruit cytoplasmic proteins in order to build a strong connection between actin and the ECM as the lamellipodium continues to push forward^{29,32}. At peak maturation, the lamellipodium has passed these more stable adhesions entirely to be replaced by a region called the lamella. In the lamella, actin becomes organized in bundles through myosin-dependent mechanisms, and adhesions elongate and grow into mature focal adhesions (FAs)^{29,32}. Once the cell body has passed these mature FAs (now at the rear of the cell), the FAs disassemble, allowing directional movement to continue³². While the actions of actomyosin networks are responsible for membrane protrusion and force generation, FAs are required to translate this force into traction to achieve motion³². Furthermore, bi-directional communication between the actin cytoskeleton and FAs is necessary for cells to both influence and respond to their environment; increasing cellular contractility promotes FA growth and maturation, while ECM-originated signals can be communicated to the cell via FAs in order to induce actin cytoskeleton remodelling and changes in cell behaviour^{32,33}.

In order to measure forces exerted by FAs on the substrate, investigators have developed a tool called traction force microscopy (TFM) in which cells are plated on polyacrylamide gels containing fluorescent beads³⁴⁻³⁶. When cells spread or migrate, they will pull on the substrate and displace the beads; given the physical properties of the gels and the magnitude of bead displacement, the traction force produced by whole cells or individual FAs can be computed³⁵. Applying TFM to single migrating cells has revealed that some FAs exhibit “tugging” dynamics,

characterized by a fluctuating traction peak along the length of the FA, which has been proposed to allow cells to probe their substrate during durotaxis (migration up a stiffness gradient)^{34,37}. This method has also been extended to higher dimensions. So-called “2.5D” TFM has been used to measure bead displacement in a 2D gel along the x-y plane and also along the z axis, revealing out-of-plane forces generated by FAs.

Extending TFM to being “truly” 3D is much more difficult for a number of reasons, including the complexity of traction field computation, 3D imaging limitations, and the construction of an appropriate substrate (reviewed in Hall et al, 2013)³⁸. Finding a 3D material in which embedded cells will spread and migrate which also satisfies the requirements of TFM methods is difficult. One possibility being explored is to replace the polyacrylamide gel component of TFM with more biologically relevant materials which allow 3D cell migration, such as collagen³⁸⁻⁴⁰. This approach comes with several drawbacks due to the fact that collagen is a complex material which responds non-linearly to force – the behaviour of collagen’s fibrous microstructure needs to be taken into account when characterizing its bulk properties, adding computational complexity to traction field reconstruction³⁸. Nevertheless, this method seems to be a promising avenue in which to pursue TFM in 3D settings more closely resembling *in vivo* cell environments, and will help to generate biologically relevant TFM measurements.

Recently, Campas et al developed a way to measure forces exerted by cells within 3D cultured epithelial cell aggregates, as well as in living embryonic tissues⁴¹. They engineered oil microdroplets approximately the size of cells, and with defined physical properties and fluorescent markers⁴¹. To introduce these into cell aggregates or tissues, they coated the surface of droplets with adhesion receptors, and upon injection these droplets would be incorporated into the sample and become surrounded by cells⁴¹. By measuring its deformation, they were able to reconstruct the

magnitude and direction of forces exerted by cells on the droplet⁴¹. This promising and highly adaptable technique could be applied in quantitative studies of cell-generated forces in a wide variety of contexts, such as development of different model organisms or within diseased tissues.

1.2.2. Collective migration and cell clusters

Single cell migration work has provided a basis to study the collective migration of cells *in vitro*, and many of the same tools, including TFM, have been applied to measure the forces exerted by a sheet of cells on their substrate^{31,42-44}. However, collective migration is inherently more complex as cell-cell forces must also be considered. In multicellular clusters (Fig. 1.3. B), cells form cadherin-based adhesions to each other, and their movement and morphology changes are regulated by forces exerted and sustained at both cell-ECM and cell-cell junctions⁴². Similarly to cell-ECM adhesions, cell-cell adhesions are responsible for transmitting forces, and also exhibit force-dependent remodelling, growth and signalling^{42,45,46}. Furthermore, cross-talk between cell-cell and cell-ECM adhesions has been demonstrated in a variety of contexts^{30,42,46,47}. For example, modulating the amount of cell-ECM adhesion can alter the balance between transmission of cell-generated forces to neighbouring cells or to the substrate³⁰. Ng et al. found that in epithelial cell clusters, forces were primarily transferred to the substrate, rather than across the cell; however, when cell-ECM adhesion was reduced by downregulating FA complex components, cell-ECM transmission decreased in favour of cell-cell force transmission³⁰.

As a result of the interplay between cell-cell and cell-ECM adhesions and forces, complex and fluctuating maps of inter and intra-cellular stresses arise in clusters of migrating cells. The orientation of these collective stresses has been shown to orient the overall direction of cell movement^{31,44,48}. Furthermore, collective migration exhibits both group and individual cell behaviours based on environmental contexts – at the leading edge of moving epithelia, “leader”

cells protrude from the group and have been shown to exert high traction forces, which dissipate with increasing distance from the leading edge^{49,50}. However, long range forces across the sheet of cells have also been detected, suggesting that cells further back do not passively follow leader cells but actively participate in migration^{31,44}. For example in the tug of war model (Fig. 1.3. C), the traction exerted by each cell is transmitted to the cells following it, resulting in a buildup of tension along the cytoskeleton and cell adhesions away from the leading edge³¹. While the mechanisms driving collective migration are still not fully understood, these cell culture models are critical to our understanding of how cell locomotion contributes to morphogenesis of a developing organism, as well as during homeostasis and disease.

1.3. Morphogenesis and cell adhesion

In order to effect morphogenetic movements, cells must form adhesions with their surroundings. Adhesion between cells is primarily achieved by homophilic interactions of the cadherin family of proteins, while adhesion to the ECM occurs through binding of heterodimeric integrin receptors to their ECM ligands. Cadherins and integrins are transmembrane proteins which bind targets outside the cell, and participate in a large variety of intracellular signaling and binding, including coupling to the actin cytoskeleton within the cell via a network of adapter proteins. While cadherins and cell-cell adhesion are critical in morphogenesis⁵¹, the focus of this work is on integrins and the role of cell-ECM adhesion in generating and regulating mechanical forces during development.

1.3.1. The integrin adhesion complex

The integrin family of transmembrane receptors form the primary link between cells and the ECM. Integrins are highly conserved, heterodimeric, transmembrane receptors composed of one α and one β subunit with large extracellular domains and small cytoplasmic tails⁵². Integrin

function is primarily regulated by switching between active and inactive states – this regulation is critical in certain tissues, for example platelets, in which unsolicited activation could result in dangerous clotting and thrombosis⁵². In the inactive state, the α and β subunits are folded over in a bent conformation; upon activation by ligand binding or through intracellular signaling via the cytoplasmic domain, the two subunits separate and unfold to take on an extended conformation⁵². In the extended conformation, integrins have increased affinity for ECM ligands, and can recruit signaling partners within the cell⁵². The ability of integrins to be activated and subsequently bind components both within and outside the cell provides the basis for two important modes of signalling: “inside-out” and “outside-in”^{52,53}. This allows integrins to respond to extracellular signals by activating, resulting in changes in cytoplasmic binding partners, and thus changing the signalling environment within the cell (outside-in signalling). Alternatively, signalling molecules under transcriptional or mechanical control within the cell can influence integrin activation, allowing them to form or enhance bonds with ECM ligands (inside-out signalling)^{52,53}.

In mammals, 18 α and 8 β subunits combine to form 24 different integrins, allowing them to control a large variety of processes within different cells and tissues⁵². In *Drosophila*, only 5 α and 2 β subunits are still implicated in a wide variety of processes throughout development and adult life^{51,54}. The most widely expressed β integrin subunit in *Drosophila* is called β PS or *myospheroid* (*mys*). The ability of integrins to mediate so many different functions is achieved not only by specialized combinations of subunits, but also by a network of adapter and signaling proteins which can regulate integrin function. The complex of the integrin receptor and the network of associated proteins is known as the integrin adhesion complex (IAC). Among these is the linker protein talin, a master regulator of integrin function, which provides a direct link between integrins and actin, and orchestrates the assembly of the intracellular adhesion complex. While most

vertebrates have 2 forms of talin, the *Drosophila* genome encodes only 1 version, which is highly homologous to vertebrate talin⁵⁵.

Talin is a large cytoplasmic protein composed of a head and a rod domain. Talin can directly bind to integrins via 2 distinct binding sites in the head and rod, as well as a suite of IAC proteins via binding domains throughout its length⁵⁶⁻⁶⁰. The rod domain of talin is composed of helical bundles – in response to pulling force, these bundles can separate like a spring, revealing cryptic binding sites⁶¹. This mechanosensory behaviour allows for additional recruitment of molecules, such as vinculin, which can reinforce adhesion in response to increased tension⁶¹. The activity of talin is also regulated through intramolecular mechanisms and through interactions with signaling molecules. The rod domain of talin includes an intramolecular binding site which binds the talin head causing the protein to take on a folded conformation, thus rendering the molecule inactive^{62,63}. This method of self-regulation is referred to as autoinhibition, and has been shown to play important regulatory roles in variety of contexts^{57,64}. Talin activity is also subject to regulation by the small-GTPase Rap1 and the Rap1-GTP-interacting adapter molecule (RIAM) – RIAM provides a scaffold to link talin, specifically in its autoinhibited conformation, to the membrane targeting sequences of Rap1, allowing talin to move to the membrane when autoinhibition can subsequently be relieved through interactions with the membrane⁶⁵⁻⁶⁷. This provides a means by which to quickly and specifically mobilize talin to sites of adhesion in order to activate integrins and promote cell-ECM adhesion.

1.3.2. Integrin-mediated adhesion in cell culture

A significant part of our knowledge of integrin function comes from the study of FAs in 2D cell culture. FAs are integrin-mediated adhesion sites formed by cells cultured on substrates containing ECM ligands. They act as structural links as well as signaling hubs, controlling cell

behaviours such as growth, proliferation and migration⁶⁸. The formation of FAs is tightly linked to actin cytoskeleton remodelling – when Rho stimulates contractility, actin is pulled into bundles or “stress fibers”, causing clustering of integrins into FAs⁶⁹. Rho is a small GTPase which participates in myosin light chain phosphorylation in order to increase contractility – this activity is opposed by another GTPase, Rac, which decreases contractility⁷⁰. The application of force also promotes the recruitment of FA associated proteins, such as talin, vinculin and paxillin²⁹. The resulting complex of proteins participate in FA responses to intra- and extracellular cues such as actomyosin contractility, externally applied tension and ECM rigidity^{34,69,71}.

High-throughput studies have revealed hundreds of interacting proteins comprising the IAC^{72,73}. Using different combinations of these IAC proteins, FAs are able to respond to a huge variety of chemical and physical stimuli and to transmit signals or remodel themselves accordingly⁷³. For example, in response to changes in contractility, a variety of mechanosensitive IAC proteins including talin and zyxin, can undergo conformational changes or relocalization in order to either strengthen adhesions or recruit new binding partners^{61,74,75}. Super-resolution microscopy work has revealed the orientation and exact position of certain IAC components within FAs: proteins are organized in layers spanning the distance from the membrane to the actin cytoskeleton⁷⁶. The first layer, proximal to the membrane, contains integrin cytoplasmic tails, the scaffolding protein paxillin, and focal adhesion kinase, which doubles as a scaffold and signalling molecule⁷⁶. The final layer, proximal to actin, contains zyxin and α -actinin, proteins involved in connecting actin filaments to FAs⁷⁶. Spanning the distance between these layers are talin, which binds both integrin and actin, and vinculin, which binds talin and actin and serves to reinforce adhesion⁷⁶. The orientation of talin, with the N-terminal head region towards integrins and the C-terminal rod region towards actin, results in a stereotyped localization of its binding sites, perhaps

guiding the stratified architecture of FAs. By building a detailed map of interacting proteins and their localization and roles within FAs, we can move towards an understanding of how integrin-based adhesions control cell behaviour both *in vitro* and *in vivo*.

1.3.3. Integrin-mediated adhesion in *Drosophila* embryogenesis

Integrin and talin are both required for *Drosophila* embryogenesis – the earliest defects exhibited in null mutants are seen in mid embryogenesis during germband retraction (GBR)^{51,55}. After axis elongation (germband extension in *Drosophila*), the germband is curved over the posterior end onto the dorsal side of the embryo. During GBR, coordinated efforts of the germband and neighbouring tissues pull the germband posteriorly and ventrally, revealing a dorsal hole (Fig 1.2. A-A''). The dorsal hole is occupied by the amnioserosa (AS), an extra-embryonic tissue which adheres to the yolk cell and to the surrounding epithelium. Following GBR, the epithelial sheets on either side of the AS migrate towards each other to form a seam and close the hole, in a process known as dorsal closure (DC) (Fig 1.1. B-D'; described in greater detail in section 1.1.1.). The AS adheres to a laminin-rich layer of ECM on top of the yolk – in the absence of integrin, the AS detaches from the ECM, highlighting the importance of integrin-mediated cell-ECM adhesion in the process⁷⁷.

Integrin and talin null mutants show defects in GBR and DC, as well as in later stages at muscle attachments. Furthermore, structure-function studies have shown that various domains of integrin and talin are important for different aspects of integrin-mediated adhesion during *Drosophila* development. Deactivating integrins by inhibiting their ability to bind ECM or signaling molecules, or by preventing ligand-binding induced conformational changes results in GBR, DC and muscle attachment defects⁷⁸. Interestingly, activating integrins by promoting talin

binding or disrupting association between integrin subunits can also cause DC and muscle attachment defects⁷⁸.

As talin is the primary regulator of integrin function, many of its binding domains and activities have been shown to be important for integrin-dependent events during embryogenesis. For example, the two integrin binding sites (IBS-1, located in the head domain, and IBS-2, in the rod) of talin appear to play different roles in development – while both are sufficient to recruit talin to integrins and are required for proper muscle attachment, only IBS-2 is required for GBR and DC⁵⁹. The difference in their roles is attributed to the different modes in which they regulate integrin function. IBS-1 is primarily responsible for maintaining integrin binding to the ECM and promotes stable adhesions, while IBS-2 supports integrin binding to talin and other IAC components and allows for dynamic adhesions⁵⁹. Structural rearrangements involved in DC and GBR require malleable adhesions and therefore IBS-2 function, while developing muscle attachments require both dynamic and stable adhesion for their formation and maturation⁵⁹. Studies have also shown that the talin head is indispensable for *Drosophila* embryogenesis, and that headless talin mutants have a high penetrance of GBR, DC and muscle attachment defects⁵⁸. Given that the phenotype of headless talin is far more severe than that of IBS-1 mutants, the talin head must participate in other facets of integrin adhesion critical for development. For example, interactions between lobes of the talin head have been shown to play a role in integrin clustering, which increases avidity for the ECM and reinforces integrin-mediated adhesion⁵⁸. Taken together, these results suggest that a careful balance must be maintained between reinforcing and turning over adhesions during morphogenetic movements.

Maintaining proper levels of talin activity is also critical for the regulation of cell-ECM adhesion during development. Previous work has shown that embryos expressing a mutant form

of talin incapable of autoinhibition exhibit increased talin recruitment and more stable adhesions – a similar effect can be achieved by expressing a constitutively active form of Rap1⁵⁷. As result of this increased integrin-mediated adhesion, embryos experience DC defects, suggesting that too much talin activity can hinder morphogenesis⁵⁷. Once again, the importance of maintaining a balance between stable and dynamics adhesions during morphogenesis is evident.

The interaction between talin and actin has also been shown to be critical for development – while preventing talin binding to actin does not affect integrin localization or ECM binding, it causes defects in GBR and DC, and results in abnormal muscle attachment architecture⁶⁰. These phenotypes are likely due to an uncoupling of force-generating mechanisms within the cell and the adhesion between cells and their surroundings. If changes within the actin cytoskeleton are not communicated to integrins via talin, remodelling of adhesions in response to cell shape changes or tensile force is abrogated, resulting in morphogenetic defects. These results suggest that mechanosensation by talin may have important roles in development, however this has yet to be directly tested *in vivo*.

1.3.4. Integrin-mediated adhesion in embryogenesis of other model organisms

The importance of integrin-mediated adhesion during development has also been demonstrated in other model organisms. For example, embryogenesis of *Xenopus laevis* involves a variety of cell-ECM adhesion-dependent cell migration and rearrangement events^{79,80}. During *Xenopus* gastrulation and epiboly, germ layers are specified while simultaneously thinning and spreading over the surface area of the embryo. Throughout this process, a fibronectin matrix is assembled between tissue layers, and the presence of this ECM layer, as well as its interaction with integrins, is required for intercalation of cells during tissue thinning and extension^{79,80}. While intercalation is typically thought of as a cadherin-dependent process, work in *Xenopus* explants

has revealed that integrin-fibronectin interactions are required to modulate cell-cell adhesion between intercalating cells, promoting their rearrangement⁸⁰. Integrin- and fibronectin-dependent collective cell migration has also been observed in the extension of the mesendoderm during epiboly, where leading edge cells develop actin-rich protrusions and all cells exert traction on the ECM⁸¹. Furthermore, integrin-fibronectin interactions have been shown to control the extent and direction of cell protrusive behaviour⁸². More recently, focal adhesion kinase has also been shown to control cell protrusions and traction forces during mesendoderm migration⁸³.

Several morphogenetic processes in *Danio rerio* (zebrafish) development have also been shown to involve integrated-mediated adhesion. For example, integrin function has been shown to play a role in somitogenesis, the process whereby groups of mesodermal cells (somites) bud off of the migrating paraxial mesoderm along the AP axis of an embryo undergoing convergent extension⁸⁴. Loss of integrin function results in somite defects, including failure of cells to undergo epithelial to mesenchymal transitions as well as failure to assemble fibronectin matrices^{84,85}. The proper assembly of fibronectin matrices is critical as it provides mechanical coupling between developing tissues⁸⁶. When integrin-fibronectin interactions are prevented, adhesion between the paraxial mesoderm and the adjacent notochord is affected, resulting in altered tissue mechanics and defects in trunk elongation in the zebrafish tail bud⁸⁶. These studies in frog and zebrafish, among many others including work in mouse and chick embryos, reveal that cell-ECM adhesion has diverse and important roles during the embryonic development.

1.4. Aim and scope of thesis

While integrins are known to be required for *Drosophila* embryogenesis, there is still much to learn about the mechanisms by which they contribute to the driving forces of morphogenetic events. In contrast, work in cell culture has been used to quantify with great precision the forces

exerted by cells on their neighbours and substrates, thanks to controlled physical environments and advanced computational tools. The natural progression, and the goal of this work, is to attempt to integrate tools and findings from *in vitro* work and to apply them to an *in vivo* system in order to gain mechanical insight into developmental events. Specifically, the aim of my work has been to understand the role of cell-ECM adhesion in governing AS cell dynamics and tissue contraction during *Drosophila* DC.

First, I build upon previous work done in the lab in order to characterize integrin-mediated adhesion sites in the AS which we have termed Focal Adhesion-like Structures (FALS). Second, I quantify changes in cell and tissue morphology over time in the background of altered cell-ECM adhesion in order to gain insight into what aspects of AS behaviour are modulated by adhesion to the ECM. Using cell tracking and laser ablation, I examine how tissue-level forces and biomechanical properties are affected when cell-ECM adhesion is modulated. Finally, I begin to investigate the mechanical coupling between neighbouring cells, as well as between cells and their substrate, in an effort to understand how force transmission in the AS might be regulated via integrin-mediated adhesion. Overall, I seek to build from lessons learned in cell culture work to understand how cell and tissue-level forces are generated and coordinated in the context of a living, developing organism.

Chapter 2: Materials and methods

2.1. Fly stocks and genetics

β PS-integrin mutants were generated using the Dominant Female Sterile germline clone technique⁸⁷ to remove both maternal and zygotic contributions of the *mys* gene product and a β PS-integrin null allele, *mys*^{XG43}, recombined onto an *FRT101* chromosome. Females of the genotype *mys*^{XG43}, *FRT101/OvoD1*, *FRT101* were subjected to a heatshock regime in the larval stages to generate *mys* mosaic germline and subsequently were crossed to wild type males with fluorescently-marked X chromosomes. Mutant embryos were identified by lack of the fluorescent marker. Embryos carrying the fluorescent marker (ie. heterozygous *mys/+* siblings) were used as controls. For live imaging experiments genomically-tagged *DE-Cad-mTomato*, *DE-Cad-GFP*, *Basigin-GFP* (Bsg-GFP)⁸⁸ and *Ubi>nls-RFP* were zygotically provided

Talin(E1777A) embryos were generated by rescuing talin-null (*rhea*^{79a} allele⁵⁵) germline clone embryos with a maternally-provided, ubiquitously-expressed, talin(E1777A) rescue construct. Females of the genotype *hs-Flp/+; pUbi-talinGFP-E1777A* or *pUbi-talinGFP-WT/+; rhea*^{79a}, *FRT2A/OvoD1*, *FRT2A* were subject to a heatshock-regime during the larval stages to generate *rhea* mosaic germline. Virgins were then crossed to *rhea*^{79a}/*TM3,Sb,dfd-GMR-nvYFP*. Embryos without the fluorescent balancer were selected for analyses. The wild-type rescue construct (talinGFP) was used as a control. Using this approach we find that WT talinGFP rescued embryos resemble WT embryos and that over-expression of transgenic talin does not cause any deleterious effects or ectopic integrin signaling⁵⁹.

Rho1-DN (Rho1-N19 Bloomington line 58818), Rho1-CA (Rho1-V14, Bloomington line 7330), Rac1-DN (Rac1-N17 Bloomington line 6292), and Rap1-CA (Rap1Q63E; see ref⁵⁷) were all expressed using the UAS/Gal4 expression system and the c381 tissue driver (gift of Nick

Harden), which is well known to be provide amnioserosa-specific expression in the embryo. Embryos expressing the driver alone were used as controls where necessary.

2.2. Live imaging

Embryos were dechorionated in 50% bleach for ~4 minutes and staged according to the criteria of Ellis et al⁵⁷. Embryos were then aligned and glued to a 1mm coverslip using embryo glue (Scotch double-sided tape dissolved in heptane), dorsal side down. Coverslips were mounted in halocarbon oil (Sigma) on glass slides with a cover-slip bridge to prevent compression of the embryos.

Images were collected using either an Olympus FV1000 inverted laser scanning confocal microscope with a UplanFL N 40x 1.30 NA oil objective or a UplanSApo 60x 1.35 NA objective, or a Zeiss Axiovert 200M spinning disk confocal microscope using a 63X 1.40 NA or 100X 1.45 NA objective. All images were acquired maintaining consistent laser power, gain, offset, and exposure time settings between control and experiment embryos to allow for direct comparison. For movies that measured closure time and/or tracked nuclei, 25-30 1.0 μm confocal sections were collected at 2-5-min intervals for a minimum of 2 hours using the 40x lens and a 473 nm (closure time) or 559 nm (nuclei tracking) laser. For movies of cell behaviour, 5-10 1 μm confocal sections were collected at 20-second intervals for a 20 minute time period. For FALS-tracking, we collected 4-8 0.5-1 μm confocal sections at 10-second intervals over 10 minutes. At least 5 movies were taken of each genotype. For movies of cell-ECM interactions (Basigin-GFP and DE-Cad-mTomato), 15-25 1 μm confocal sections were collected at 10 or 30 second intervals for a 10 minute time period.

2.3. Laser ablation

Laser ablation experiments were carried out using a Revolution XD spinning disk confocal microscope equipped with an iXon Ultra 897 camera (Andor) and a 60× oil immersion lens (Olympus, NA 1.35). Ablation was induced using a pulsed Micropoint N2 laser (Andor) tuned to 365 nm. Z-stacks were acquired every 3 seconds for up to 60 seconds following ablation. Cuts were performed at the onset of the slow phase of DC for Talin(E1777A), Rap1-CA and *mys* ^{-/-} embryos. For wild-type characterization, cuts were performed before (early) and after the onset of the slow stage (mid). See Blanchard et al (ref ¹²) for a description of the phases of DC.

2.4. Image analysis

2.4.1. Closure rate, AS shape and cell extrusion

AS outlines were traced manually using ImageJ or MatLab, and then processed using custom scripts written in MatLab to calculate total AS area over time. To determine rate of closure curves fit to the exponential

$$A(t) = A_0 e^{-kt}$$

Where A is area, A₀ is initial area, k is the rate of closure, and t is time.

In the analysis of tissue shape over time, closure curves were aligned based on raw values of area. Perimeter, width (AP length) and height (ML) were all computed from the AS outlines, and used to calculate aspect ratio (width divided by height).

2.4.2. FALS morphology and tracking

We developed automatic image segmentation and analysis tools in MatLab to obtain estimates for FALS area, density and intensity (Fig 2.1). Briefly, single slice images of the basal portion of AS cells were filtered using a difference of Gaussians approach, in which two different widths of filters are applied to images and the difference between them is used as the final filtered

image. We used a wider filter to remove background noise and a smaller filter with a width comparable to FALS in order to remove smaller objects. The filtered images were then thresholded and applied as masks to the original images. Bright spots within a specified size tolerance were then identified, and subsequent area and pixel intensity was determined. Density was calculated as the number of FALS in an image divided by the image area.

Single FALS were tracked using a custom-developed set of algorithms in MatLab. This script automatically identifies FALS as described above, then locates the nearest FALS in the following frame and records the centroid coordinates over time. If no FALS were found within a certain search radius, trajectories were ended. Image drift was accounted for by computing the cross-correlation of subsequent frames and subtracting their offsets from trajectories.

2.4.3. Cell morphology and movement

Cell outlines were obtained using two methods: (1) movies labelled with DE-Cad-GFP or DE-Cad-mTomato were processed in SIESTA⁸⁹ using watershed and LiveWire segmentation algorithms and (2) movies labelled with TalinGFP were processed manually using ImageJ because the marker localizes basolaterally and is too noisy for automated image segmentation tools. All cell outlines were processed in MatLab to calculate cell area and centroid over time. Cell area curves were detrended to determine amplitude and period of oscillations. Cell centroid was calculated as the mean of all (x,y) coordinates of the outline.

Mean cell centroid speed was computed as the average magnitude of centroid displacement between frames divided by the time step. Mean radius of trajectory was computed as the average distance between each point and the midpoint (average of all points in the trajectory). Range of movement was calculated as the ratio of mean trajectory area ($\pi * \text{mean radius}^2$) to mean cell area for each cell.

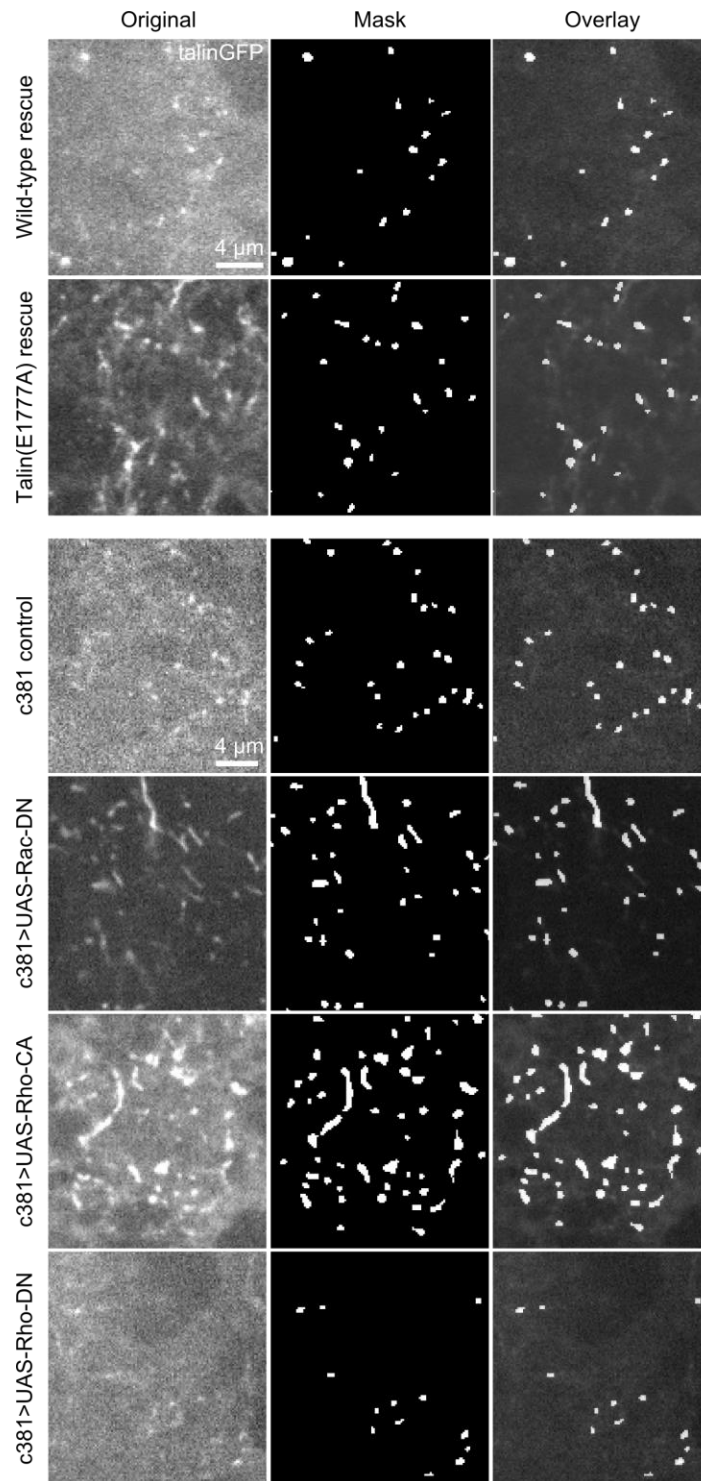


Figure 2.1. Automatic segmentation of FALS in the AS.

Original (left), automatically generated mask (middle), and overlay of mask on original (right) for various mutant lines used during this project.

2.4.4. MSD analysis

MSD analyses of FALS and of cell centroids were performed in the same way. MSD curves were computed according to the equation

$$MSD(\tau) = \langle |\vec{r}((t + \tau) - r(t))|^2 \rangle$$

where t is time, r is the displacement vector and τ is the trajectory length. These lines were then fit to the equation

$$MSD = 4D\tau$$

where D is the diffusion constant and τ is the trajectory length.

2.4.5. Cell movement correlation

To correlate cell centroid movement of pairs of AS cells, we first isolated individual cell movement by subtracting the mean movement of all cells. We then computed the cross correlation of each pair's movement using the MatLab function *crosscorr*, to apply the following equation:

$$r_{d_1, d_2}(k) = \frac{\sum_t (d_1(t) - \bar{d}_1)(d_2(t - k) - \bar{d}_2)}{\sum_t (d_1(t) - \bar{d}_1)^2 \sum_t (d_2(t - k) - \bar{d}_2)^2}$$

Where r is the cross correlation as a function of the time lag k , and d_1 and d_2 are the displacements of each cell as a function of time t . The analysis was done in 800s long blocks along the time course of each movie. Cells were considered first neighbours if their centroids were within 15 μm of each other, and second neighbours if their centroids were between 15 and 30 μm apart.

2.4.6. Nucleus tracking

We developed semi-automatic tracking tools in MatLab to analyse movies of DC to track the movement of cell nuclei. This was done either with embryos expressing ubi-nls-RFP or talinGFP. In the talinGFP case, nucleus tracking was possible because talinGFP signal is visible

everywhere except the nucleus. Movies were inverted and then filtered using the difference of Gaussians approach before the tracking algorithm was applied. Single nuclei were tracked one at a time over 20 frames (40 minutes), and a minimum of 10 nuclei per region/stage, per embryo were tracked. To compare spatial and temporal differences in cell movement, we divided the AS into inner (more than 3 cells from the edge) and outer (within 3 cells from the edge) regions, and into early (pre-AS contraction) and mid (post-onset of contraction) stages. Image drift was accounted for as described above, and all subsequent analyses were performed using custom scripts in MatLab to calculate the magnitude and direction of their displacement vectors over 20 minute intervals.

2.4.7. Recoil after laser ablation

Movement of first and second neighbour junctions was measured using SIESTA⁸⁹. First neighbours are defined as junctions immediately adjacent to the cut, while second neighbours are the two junctions next to each first neighbour. Far, or $\geq 3^{\text{rd}}$ neighbours are junctions at least one membrane segment further than second neighbours. Recoil velocity was determined by the displacement of junctions immediately after the cut. Maximum displacement was measured as the maximum distance from each junction to the midpoint between first neighbour junctions immediately prior to the cut. Spatial decay was measured as the slope of the line of best fit of maximum displacement as a function of the junction's distance from the midpoint before ablation. Image drift was accounted for by computing the cross-correlation of subsequent frames and subtracting their offsets from trajectories.

To apply models of recoil, we measured the change in distance between the junctions adjacent to the cut for 1 minute following ablation. Distance typically increased and then reached a plateau - if distance began to decrease substantially, the series was truncated in order to ensure a

better fit. The data was then fit using a non-linear least squares fitting procedure with two different 2-parameter models. The exponential model^{90,91} follows the equation:

$$d(t) = \frac{T}{\xi} \left(1 - e^{-\frac{\xi t}{\eta}}\right)$$

Where $d(t)$ is junction distance over time t , T is tensile force, ξ is stiffness and η is viscosity. Using this equation, we can solve for the maximal displacement T/ξ and the decay time constant η/ξ . The power law model^{90,91} follows the equation:

$$d(t) = Dt^\alpha$$

Where D is related to the extent of displacement and α is the fluidity. If α is closer to 1, the tissue is more fluid-like, and if it is closer to 0, it is more solid.

2.4.8. Cell-substrate movement correlations

In order to measure in-plane substrate movement, particle image velocimetry (PIV) was implemented using custom-written MatLab scripts based on the approach described by Levayer et al.⁹² to track the movement of Bsg-GFP intensity. Images were divided into 16 x 16 pixel windows overlapping by 50%, so that their centers were 8 pixels apart. We then computed the 2D cross correlation of each window in subsequent frames of the movie to determine the direction and magnitude of intensity movement. To determine cell movement, we used the DE-Cad-mTomato channel and made cell outlines in SIESTA. To isolate PIV vectors corresponding to each cell, we determined which interrogation windows had a minimum of 2 vertices within the cell contour at each time point, generating a cell-specific PIV data set. Substrate movement was then defined as the sum of the x (AP) and y (ML) components of all vectors within the cell. To control for overall substrate movement, we computed the mean displacement of the entire visible field of Bsg-GFP

intensity between each time step, and subtracted this from each vector within a cell and from the cell's displacement. Cross correlation of substrate movement and cell centroid movement was computed using the equation in 2.4.5. The analysis was done in 150s long blocks along the time course of each movie.

To measure out-of-plane, or dorsal-ventral (DV), substrate movement, we used the same time-lapses as above, and devised an approach to estimate substrate height. We divided the z-stacks for each time point of the Bsg-GFP channel into 4x4 pixel windows (in the x-y plane, i.e. 4 x 4 x n_z rectangular prisms, where n_z is the number of z slices) overlapping by 50%. For each 1 x 1 x n_z column in the window, we found the z-coordinate of maximum Bsg-GFP intensity. We then computed the median z-coordinate for all 4 columns, which was stored as the substrate height for that window, generating a down-sampled map of substrate heights across the image. We chose this approach in order to reduce noise, since the Bsg-GFP signal is not homogeneous along x and y. To generate cell-specific substrate height data sets, we determined which windows were entirely contained within the cell outline as measured by DE-Cad-mTomato and SIESTA. The mean substrate height within that cell was then defined as the mean of z-coordinates associated with all windows in the cell. Before computing cross-correlation of cell area fluctuations and z-displacements, we accounted for z-drift of movies. We performed a linear fit of z-height over time to determine the average slope of z-movement for each time-lapse, and then detrended the z-height curves for each cell according to the average trend in z. This preserved z-fluctuations, but removed drift. We then computed the change in area:

$$\Delta A = \frac{A(t + 1) - A(t)}{dt}$$

where A is area, t is time and dt is the time step, and change in z height:

$$\Delta z = \frac{z(t + 1) - z(t)}{dt}$$

where z is the z -coordinate of mean substrate height. We determine the cross correlation of ΔA and Δz using the same equation as in 2.4.5, in 180s long blocks along the time course of each movie.

2.5. Mathematical model of DC

The mathematical model used is described in Wang et al¹³. We changed only the friction factor (η) from the published value of 100 in increments of 10 between 80 and 200, ran the simulation, and used the output tissue and cell areas to generate closure curves and to compute closure rate. Vertex coordinates were used to calculate cell centroid movement. Only the time points at the beginning of the model, before cell ratcheting began, were used in our calculations in order to reflect the experimental data.

Chapter 3: Results

3.1. Focal adhesion-like structures in the AS

Integrins are enriched in the basal domains of AS cells, and the main DC defect observed in integrin mutant embryos is loss of adhesion between the basal AS and the underlying ECM that overlays the yolk⁷⁷. Previous work in our lab has shown using fluorescently-tagged transgenes that integrin and talin localize to dot-like adhesive structures on the basal surface of the AS (Fig. 3.1. A-A''). These adhesive structures share many features with FAs, thus we named them Focal Adhesion-Like Structures (FALS). Using particle tracking of FALS labelled by talinGFP, we found FALS to be dynamic and mobile (Fig. 3.1. B-B'). Furthermore, like FAs, FALS were mechanosensitive: they responded to changes in intrinsic force modulated by altering actomyosin contractility (Fig. 3.1. C-D')⁶⁹. When contractility was increased by expressing dominant negative Rac1 (Rac1-DN) or constitutively active Rho1 (Rho1-CA), FALS were larger and more dense (Fig. 3.1. C'-C'', D-D'). Conversely, when contractility was decreased using dominant negative Rho1 (Rho1-DN), FALS were smaller and less dense (Fig. 3.1. C''', D-D').

A number of mutant backgrounds have been described to either increase or decrease integrin-mediated adhesion. We tested whether FALS morphology and intensity were altered in these mutant backgrounds. A maternal-zygotic null mutation in *mysospheroid*/ β PS-integrin (*mys-/-*;⁹³) was utilized to eliminate cell-ECM adhesion. FALS were not detected in integrin-deficient embryos (Fig. 3.2. A). To increase integrin-mediated adhesion, we utilized embryos in which endogenous Talin was replaced with a mutated version that is defective in autoinhibition. It has been previously shown that this mutation in Talin (E1777A) positively regulates adhesion⁵⁷. As an alternative means to increase cell-ECM adhesion, we expressed a constitutively active version of the small GTPase Rap1 (Rap1-CA) specifically in the AS; expression of Rap1-CA gives rise

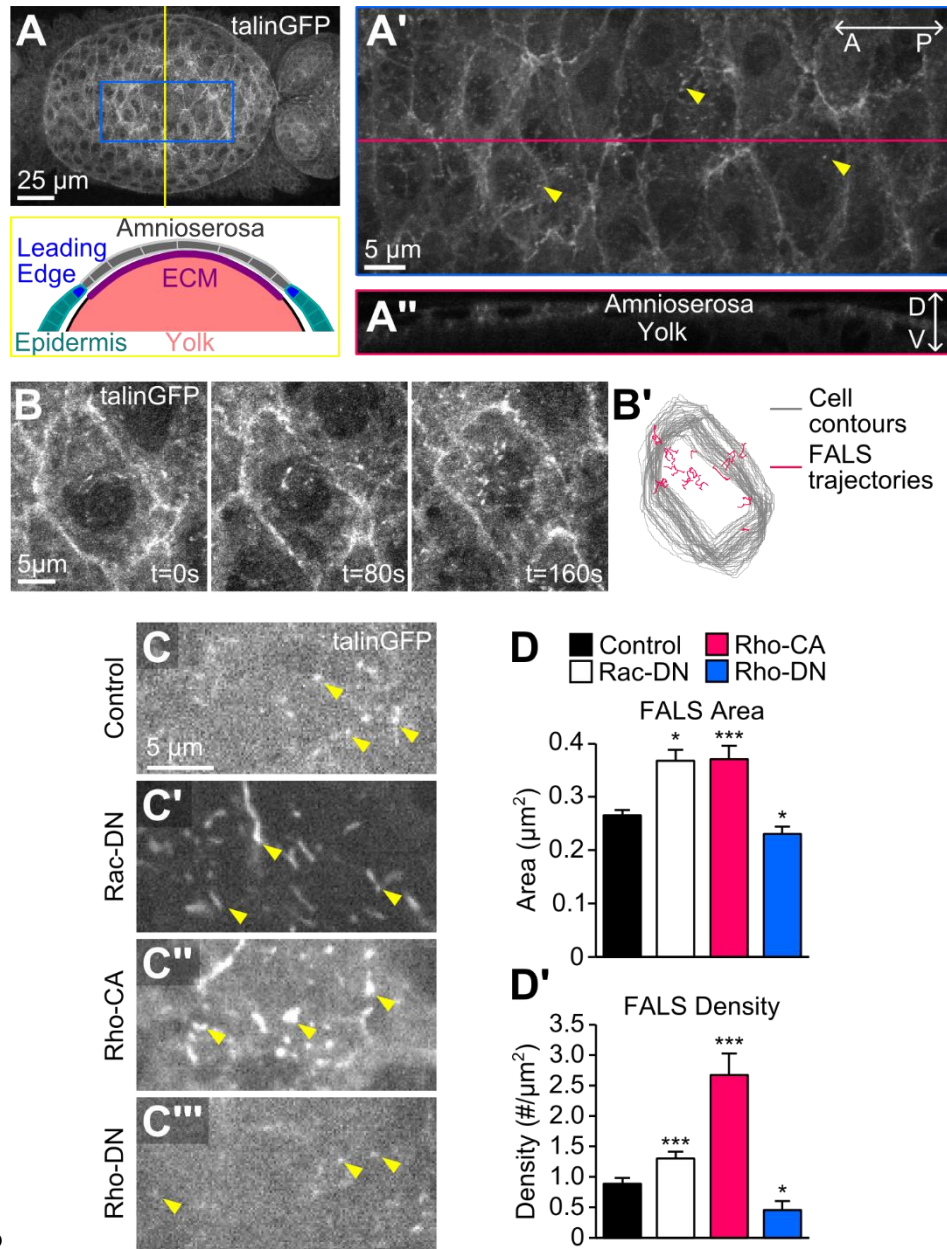


Figure 3.1. FALS are dynamic, mechanosensitive adhesion sites in the AS

(A) Image of an embryo expressing TalinGFP (top panel) and schematic of a cross-sectional view of an embryo showing the amnioserosa (AS), epidermis, leading edge, ECM and yolk. (A') Zoomed-in view of (A) showing cells and FALS in the AS. Yellow arrows indicate a subset of visible FALS. (A'') Side view of the z-stack in (A'). (B) Images from a time-lapse movie of FALS and AS cells at 0s, 80s, and 160s. (B') Overlay of cell contours (grey) and FALS trajectories (pink) from time-lapse in (B). (C-C''') Images of FALS in control embryos (C) and Rac-DN (C'), Rho-CA (C'') and Rho-DN (C''') mutant embryos expressing TalinGFP. Yellow arrows indicate a subset of visible FALS. (D-D') FALS area (D) and density (D') for controls and all 3 mutants. Error bars indicate SEM. *** indicates $p < 0.0001$, * $p < 0.05$

to increased cell-ECM adhesion⁵⁷. Consistent with the known effects of Talin(E1777A) and Rap1-CA, FALS were substantially larger and more numerous (Fig. 3.2. A-E). FAs play a critical role in cell spreading and motility *in vitro* by providing an anchor to the underlying substrate in order to transduce forces generated by actomyosin networks within the cell. We therefore asked whether FALS may play a similar role in the AS, and whether altering FALS morphology would impact cell behavior and force generation during DC.

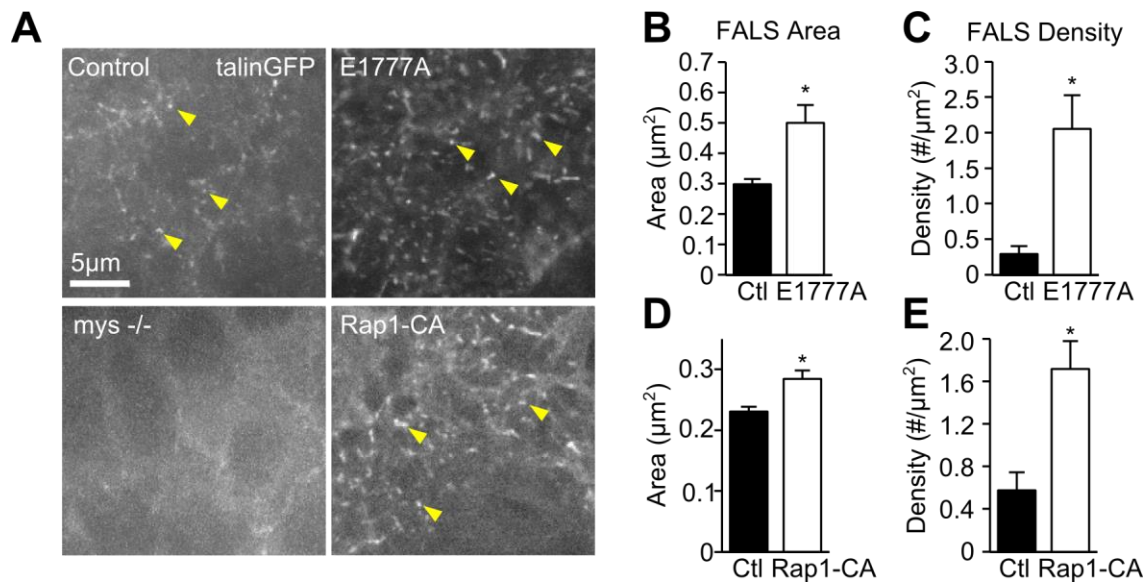


Figure 3.2. Modulating cell-ECM adhesion affects FALS morphology

(A) Images of FALS in control embryos (top left), *mys*^{-/-} (bottom left), E1777A (top right) and Rap1-CA (bottom right) mutant embryos expressing TalinGFP. Yellow arrows point to a subset of visible FALS. (B-E) FALS area (B, D) and density (C, E) for E1777A (B-C) and Rap1-CA (D-E) mutants. Error bars indicate SEM. * indicates $p < 0.05$.

3.2. Cell-ECM adhesion is required for DC

Previous work demonstrated that DC was disrupted to varying degrees in all three genetic backgrounds studied – open dorsal holes were seen more frequently in all mutant embryos than in controls at later stages of development^{57,77}. To gain more insight into how these defects arose, we performed quantitative image analysis of time-lapse movies of DC in *mys*^{-/-} embryos as well as Talin(E1777A)-rescued and Rap1-CA expressing embryos. By measuring AS area over time

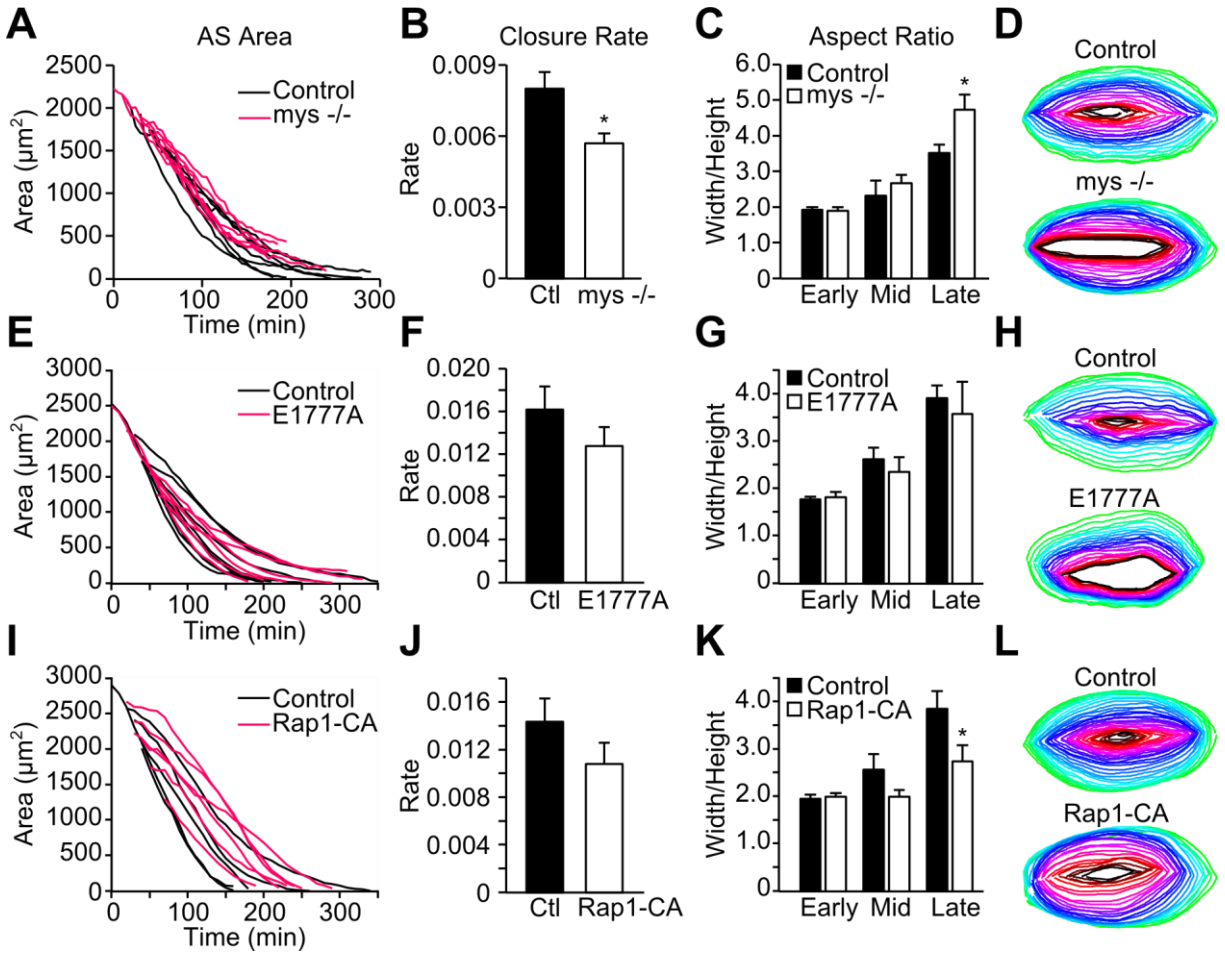


Figure 3.3. Cell-ECM adhesion is required for DC.

(A, E, I) AS area over time in *mys*^{-/-} (A), E1777A (E) and Rap1-CA mutants (I) and controls. Areas are temporally aligned based on area at the beginning of the time-lapse movie. (B, F, J) Closure rate determined by fitting areas in (A, E, I) to the function $A(t) = C \cdot \exp(-kt)$ where k is the rate. (C, G, K) Aspect ratio (width/height) at early, mid and late stages of closure. Stages are 60 minutes apart. (D, H, L) Temporal overlay of amnioserosa contours over the course of closure. Error bars indicate SEM. * indicates $p < 0.05$.

and computing closure rate, we determined that *mys*^{-/-} mutants closed at a significantly lower rate, while E1777A and Rap1-CA closed only slightly more slowly than controls (Fig. 3.3. A-B, E-F, I-J). Furthermore, we observed that the shape of the AS evolves differently over the course of closure when cell-ECM adhesion is increased or decreased. In *mys*^{-/-} mutants, the AS takes on an elongated shape, characterized by a high aspect ratio (width/height) towards the end of closure,

suggesting impaired tissue contraction along the AP axis (Fig. 3.2. C-D). While there was no significant difference in E1777A mutants (Fig. 3.3. G-H), in Rap1-CA mutants, the AS was more circular than controls, as evidenced by a lower aspect ratio in the late stages of closure, suggesting impaired ML contraction (Fig. 3.3. K-L). These results suggest that AS contraction may be affected by cell-ECM adhesion.

3.3. AS cell mobility is modulated by cell-ECM adhesion

In morphogenetic contexts, basal cell-ECM adhesion has long been correlated with cell mobility. For example, during morphogenesis of the *Drosophila* egg chamber, focal adhesion-like structures facilitate collective migration of follicular epithelial cells⁹⁴⁻⁹⁶. We asked if integrins might act in a similar capacity in the AS. We assessed whether AS cells were mobile using time-lapse imaging to track cell centroids during the early phase of DC. This analysis revealed that in wild-type embryos, AS cells did indeed move over time (Fig. 3.4. A-B). Plotting the mean square displacement (MSD) for representative cells showed that cell movement followed a pattern characteristic of random motion (Fig. 3.4. C). The movement of the cell centroid as measured here reflects both individual cell area oscillations as well as the effect of neighboring cell movement and shape changes, but not overall directional motion caused by tissue contraction.

Subsequently, cell mobility was analyzed in the mutant backgrounds where cell-ECM adhesion was modulated (Fig. 3.4. D-R). In integrin-deficient embryos instantaneous cell speed was increased, while in E1777A and Rap1-CA embryos it was decreased (Fig. 3.4. E, J, O). MSD analysis of cell trajectories revealed that cell movement was characterized by a higher diffusion constant in integrin mutants and a lower diffusion constant in E1777A and Rap1-CA mutants (Fig. 3.4. F, K, P). We also characterized the range of motion of cells by computing the mean area of

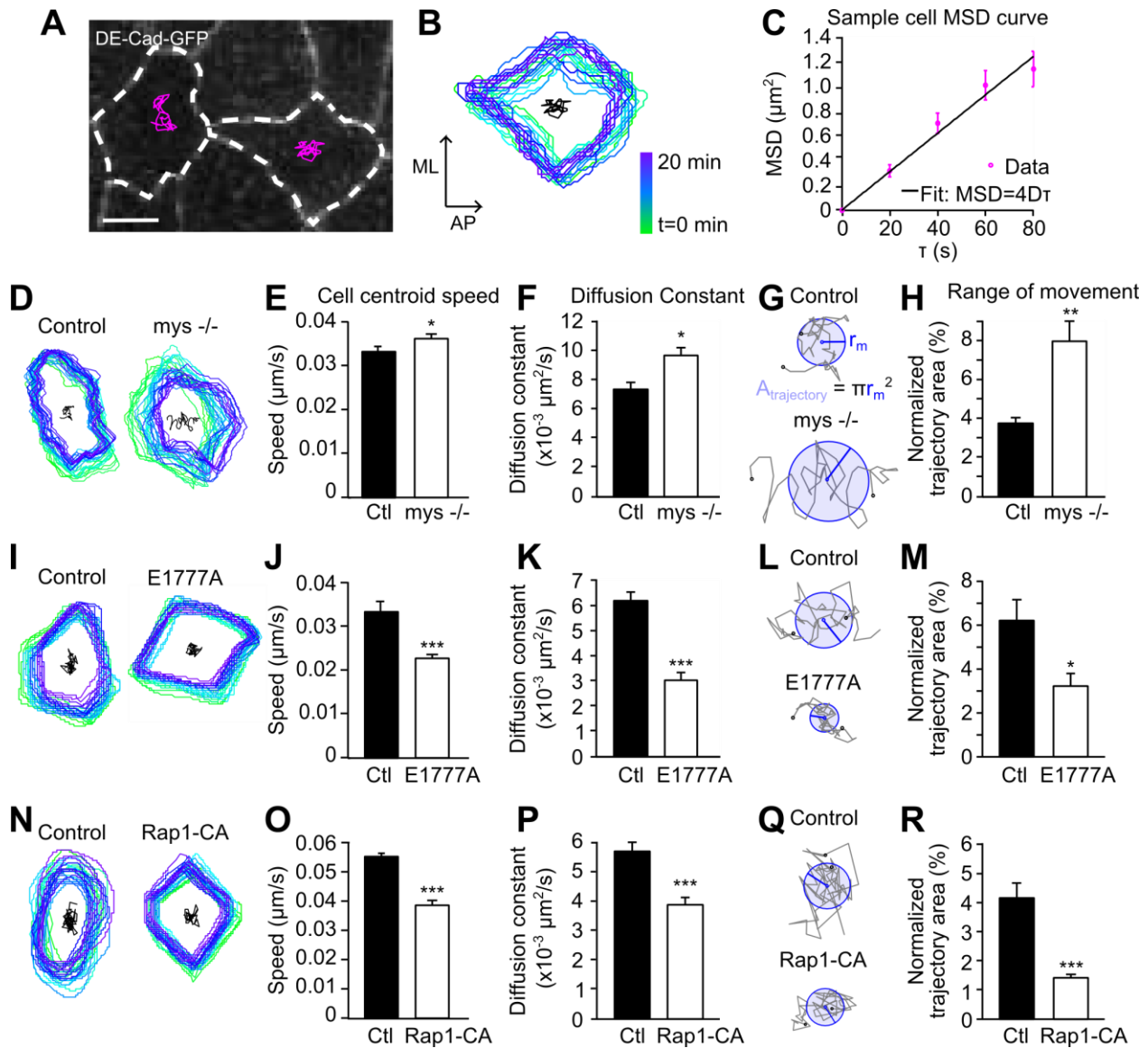


Figure 3.4. AS cell mobility is modulated by cell-ECM adhesion

(A) Wild-type AS cells labelled with DE-Cadherin-GFP with average cell movement represented by centroid trajectories (magenta). (B) Sequential overlay of AS cell contours and centroid trajectory (black) of sample wild-type cell. (C) MSD plot of cell in (B) including fit. (D-R) Cell mobility measurements and representative plots. (D, I, N) Sample AS cell contours and centroid trajectories from mutants and controls. (E, J, O) Cell centroid speed in mutants and controls. (F, K, P) Diffusion constants characterizing control and mutant cell movement estimated by fitting MSD plots for each cell. (G, L, Q) Zoom in of cell trajectories (grey) showing start and end points (small black circles), mean radius of trajectory (dark blue) and trajectory area (light blue). (H, M, R) Range of movement of mutant and control cells, computed as the trajectory area divided by the average cell area. Scale bar represents $5\mu\text{m}$. Error bars indicate SEM. *** indicates $p < 0.0001$, ** $p < 0.001$, and * $p < 0.05$.

the trajectory normalized to cell area. Integrin mutants have a larger range of cell movement, while E1777A and Rap1-CA mutants have a smaller range (Fig. 3.4. G-H, L-M, Q-R). Taken together, these data show that cell mobility in the AS and cell-ECM adhesion are inversely correlated.

One possible interpretation of this data is that misregulation of cell-ECM adhesion affects the movement of AS cells and subsequently leads to defects in DC. Since DC is a complex process involving multiple overlapping processes we sought to test this hypothesis in a simplified system. To this end we used an existing mathematical model of DC to assay the possible effects of modulating cell-ECM adhesion on cell mobility and DC. The model we employed is a cell-level

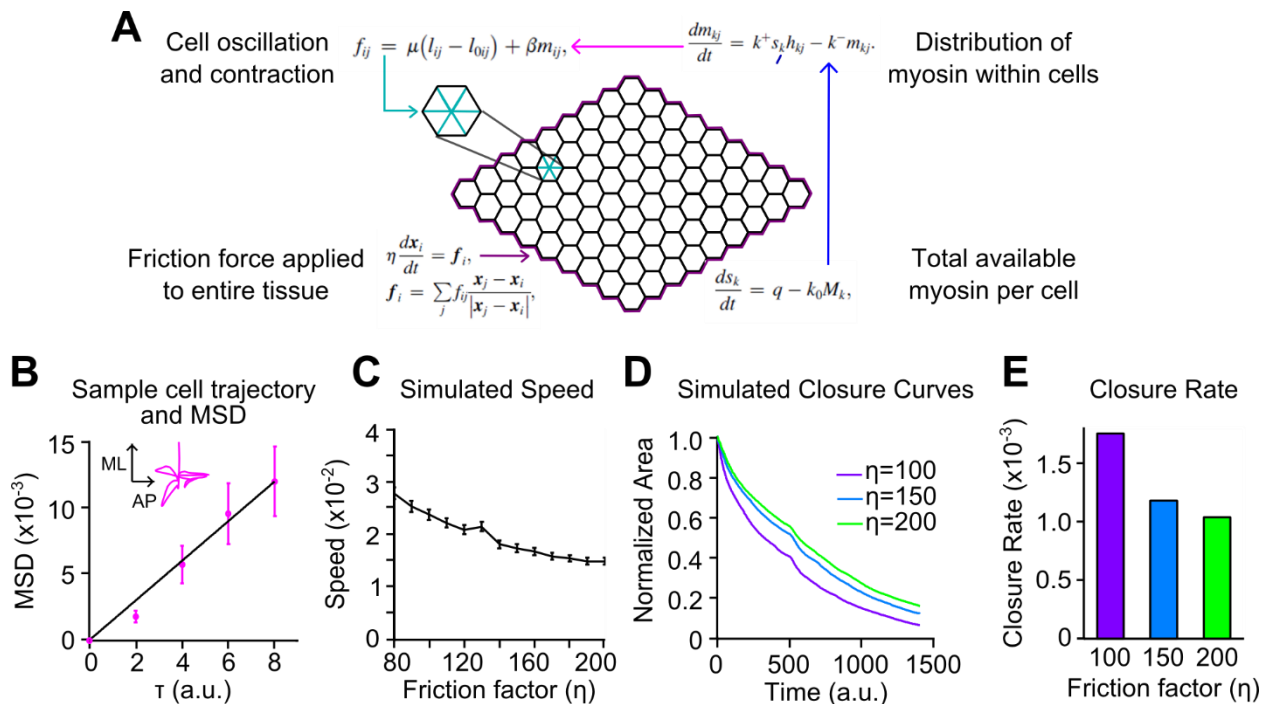


Figure 3.5. A mathematical model of DC suggests a role for friction in cell movement and closure phenotypes.

(A) Schematic illustrating the different components of a cell-level mechanical model of DC adapted from ¹³ and used to simulate DC under different conditions. (B) Sample cell centroid trajectory from DC simulation and MSD plot. (C) Velocity of AS cells from simulations with different levels of friction. (D) AS area over time and (E) rate of closure for baseline and increased friction. Error bars indicate SEM.

biomechanical model that effectively simulates the early stages of DC (Fig. 3.5. A)¹³. The model includes a friction factor, η , which opposes the movement of cell vertices. When η is manipulated to simulate the effects of increased or decreased cell-ECM adhesion, AS cell mobility is altered. Increasing friction to simulate the effects of higher cell-ECM adhesion in the AS leads to decreased cell movement in the model. In contrast, decreased friction leads to increased cell mobility (Fig. 3.5. B-C). Moreover, when friction increases the model predicts longer closure times, consistent with what we observe in embryos when cell-ECM adhesion is increased (Fig. 3.5. D-E). Therefore, the model is in line with the idea that modulation of cell-ECM adhesion regulates cell mobility within the AS and this may underlie the delays we observe in DC.

3.4. Global patterns of cell movement and tension in the AS

To gain tissue-wide insight into links between DC defects, cell-ECM adhesion, and cell mobility, patterns of cell movement were characterized across the AS over longer time periods. Using cell nucleus tracking to detect directional movement in wild-type and mutant backgrounds, we compared the magnitude and direction of cell displacement for central (“inner”) versus peripheral (“outer”) cells of the AS during early and mid stages of DC in wild-type embryos (Fig. 3.6. A). Early was defined as before the onset of closure, while mid was defined as immediately after onset, as judged by the changing shape of the canthi (Fig. 3.6. A). When the magnitude and angle of cell displacement were quantified relative to the medial-lateral axis, outer cells exhibited increasingly polarized, anisotropic motion over time while inner cell movements remained isotropic and relatively constant (Fig. 3.6. A-C, F-G).

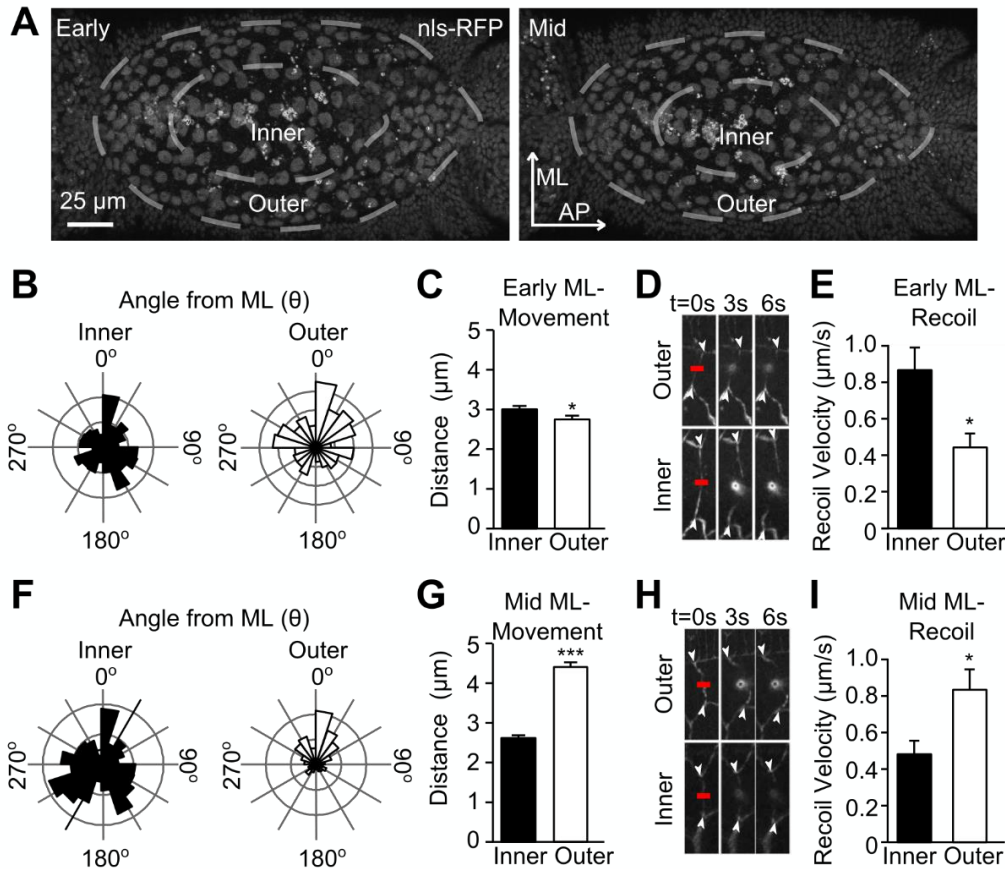


Figure 3.6. Global patterns of cell movement and tension in the AS

(A) Legend indicating inner and outer cells, axes of embryo and tissue shape at early and mid stages of closure. (B, F) Angle from ML of nucleus movement in inner (left) and outer (right) cells during early closure (B) and mid closure (F). (C, G) ML displacement of inner and outer cells at early (C) and mid closure (G) stages. (D, H) Kymographs of cell membranes before and after laser ablation in early (D) and mid closure (H) stages. Arrows indicate tracked junctions, red line indicates location of cut. (E, I) Recoil velocity of inner and outer cell junctions after laser ablation at early (E) and mid (I) stages. Error bar indicate SEM. *** indicates $p < 0.0001$, * < 0.05 .

Previous work implied that differential distribution of forces between inner and outer AS cells might contribute to closure^{97,98}, but this has never been directly assessed. We wondered if the patterns of cell movement we observed could reflect regional differences in tension. To test this idea, we set out to confirm that tensile forces were different between inner and outer regions of the AS. Laser ablation of cell membranes was used to measure the recoil velocity of adjacent cell-cell junctions following ablation as a read-out for tissue tension. This analysis revealed that in early

DC, the recoil velocity of inner cells is greater than that of outer cells indicating there is more tension distributed across inner cells in early DC (Fig. 3.6. D-E). We discovered that during mid-closure, this trend was reversed: outer cells had faster recoil velocity indicating more tension in outer cells than inner cells (Fig. 3.6. H-I). This increase in tension correlates with the observed increase in movement of outer cells during mid-DC and suggests that relative changes in cell mobility may be related to the amount of tissue tension. Our data also imply that a transition in cell behavior between early and mid-stages of DC corresponds to a redistribution of tension that is likely to be important for properly timed closure.

These changes in cell movement and tension may be a result of either altered patterns of actomyosin contractility, or of cell-ECM adhesion. Myosin levels increase in the AS during closure, suggesting contractility may increase over time¹², but we do not know how contractility evolves in different regions of the AS. To determine if cell-ECM adhesion exhibits spatial and temporal differences, we quantified FALS area, intensity, and density at early and mid closure in the inner and outer regions of the AS. We found that FALS area and intensity were constant across all groups (Fig. 3.7. A-C), while density was lower in outer cells during both early and mid-closure (Fig. 3.7. D). A lower density of FALS may result in less frictional resistance to cell movement, allowing outer cells to move more along the ML axis during mid closure. This raises the question of why outer cells in early closure, with low FALS density, do not exhibit more ML-movement. In terms of AP and total movement, outer cells in early closure do not show large net movement or directionality (Fig. 3.7. E-H), suggesting that while FALS may control cell mobility, they do not directly mediate directional movement over longer time periods – this may be controlled by changes in actomyosin contractility or tissue-level forces.

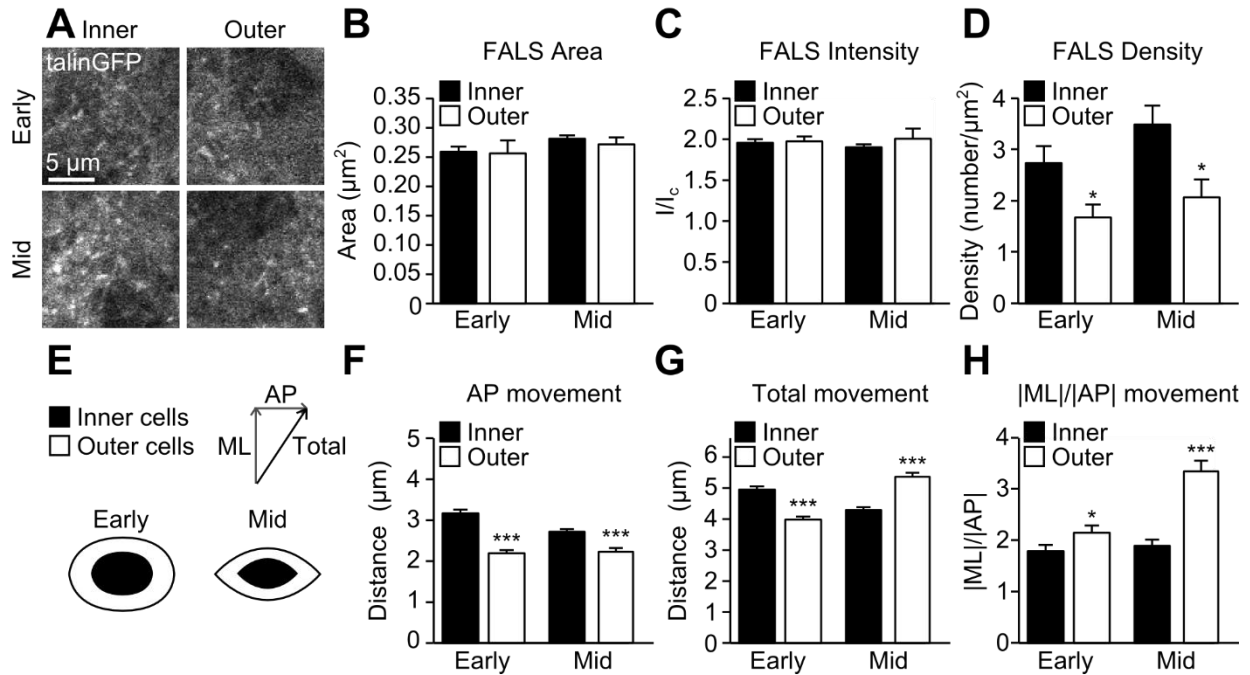


Figure 3.7. Spatiotemporal differences in cell-ECM adhesion and cell movement in the AS

(A) Sample images of FALS from early stages (top panels) and mid stages (bottom panels) in inner (left panels) and outer (right panels) regions of the AS. (B-D) FALS area, intensity and density at early and mid stages of closure, in inner and outer regions of the AS. Intensity (I) is normalized to cytoplasmic intensity (I_c). (E) Legend of inner and outer cells, early and mid closure AS shape, and ML/AP axes. (F-G) AP (F) and total (G) movement of inner and outer cells in early and mid closure. (H) Ratio of ML to AP movement for inner and outer cells at early and mid closure. A value of 1 would indicate equal movement along AP and ML, while values greater than 1 indicate ML movement greater than AP. Error bar indicate SEM. *** indicates $p < 0.0001$, * < 0.05 .

3.5. Cell-ECM adhesion regulates global AS cell movement and tissue tension

As cell mobility is correlated to both tension and the level of cell-ECM adhesion, we hypothesized that there were direct links between tension and cell-ECM adhesion. We built on this finding by extending our analysis of cell movement and tissue tension to mutant embryos in order to observe the effects of modulated cell-ECM adhesion. Cell tracking experiments in integrin mutants at mid-DC stages revealed greater ML-displacement in both inner and outer cells (Fig. 3.8. A). In E1777A and Rap1-CA mutants, outer cells exhibited lower ML-displacement than

controls (Fig. 3.8. D, G). This data suggests that when cell-ECM adhesion is decreased, there is more efficient ML-contraction of the AS characterized by more movement of cells towards the dorsal midline. However when cell-ECM adhesion is too great, cell movement and tissue ML-contraction is slowed.

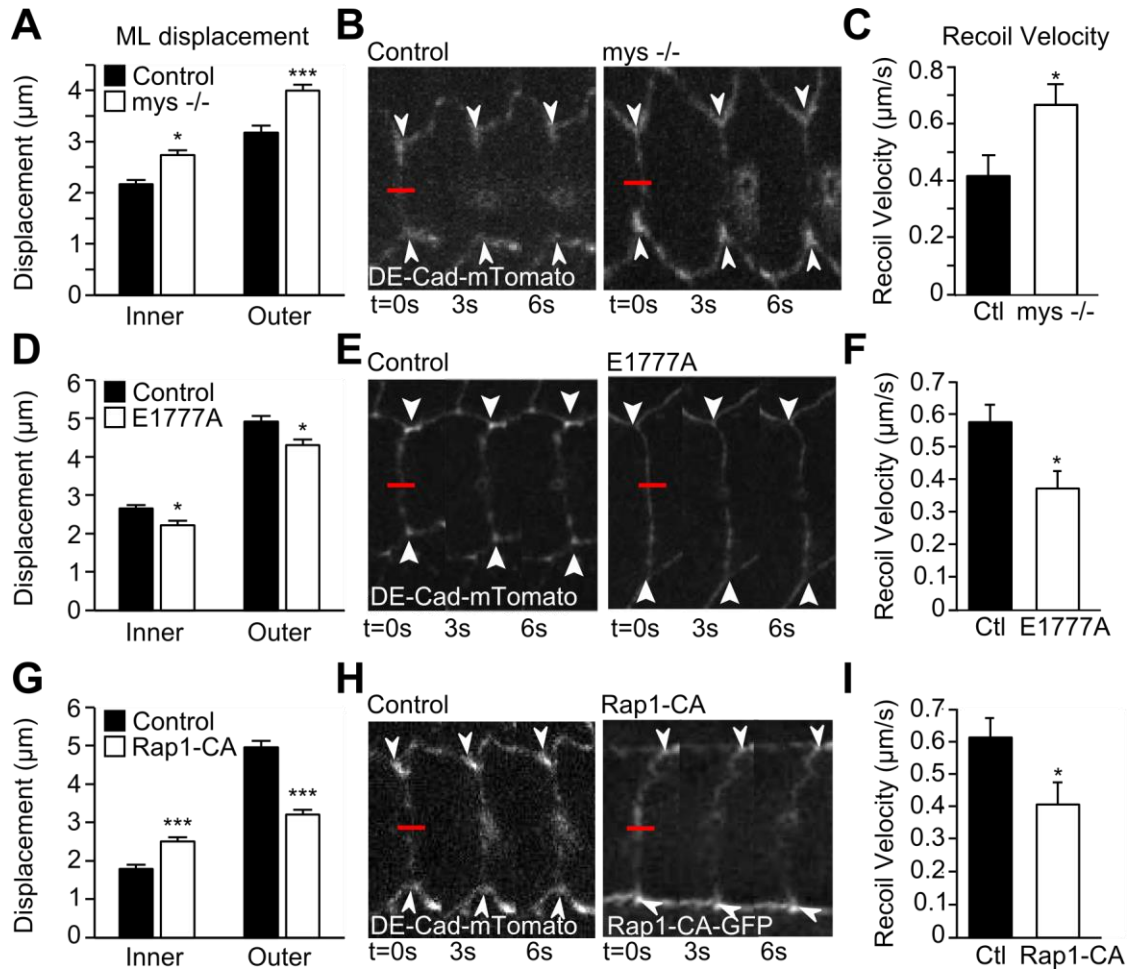


Figure 3.8. Cell-ECM adhesion regulates movement patterns and tension in the AS

(A, D, G) ML displacement of inner (black) and outer (white) cells during mid stages of closure in *mys*^{-/-} (A), E1777A (D) and Rap1-CA (G) mutants with controls as measured by nucleus tracking. (B, E, H) Kymographs of cell membranes after laser ablation in *mys*^{-/-} (B), E1777A (E) Rap1-CA (H) mutants and controls. Arrows indicate tracked junctions, red line indicates location of cut. (C, F, I) Recoil velocity of cell junctions after laser ablation in mutants and controls. Error bars indicate SEM. *** indicates $p < 0.0001$, ** $p < 0.001$, * $p < 0.05$.

To directly test the effect of cell-ECM adhesion on tension, we used laser ablation of cell membranes to measure the recoil velocity of adjacent cell-cell junctions. Cuts were made in central AS cell membranes, perpendicular to the anterior-posterior axis, to estimate tension along the medial-lateral axis. These experiments revealed higher recoil velocity and thus greater tissue tension in integrin mutants (Fig. 3.8. B-C). Conversely, in Rap1-CA and E1777A mutant embryos recoil velocity was reduced compared to controls indicating decreased tissue tension when integrin-mediated adhesion is increased (Fig. 3.8. E-F, H-I). Taken together these two lines of study support a correlation between cell-ECM adhesion, cell mobility, and tension.

3.6. Force-generation and tissue biomechanical properties in the background of altered cell-ECM adhesion

The data presented thus far demonstrates that cell-ECM adhesion regulates the mobility of cells across the AS, as well as the level of the tissue tension that must be generated and maintained for DC. Tension in the AS is generated primarily by actomyosin ratcheting of apical cell area¹⁸, Therefore, we investigated whether this process was affected when cell-ECM adhesion was modulated by examining the amplitude and period of cell area oscillations. We found that while the differences between mutants and controls were subtle, oscillation amplitude correlated inversely with the amount of cell-ECM adhesion (Fig. 3.9. A-C, E-G, I-K). However, despite a modest increase in *mys* *-/-* mutants, there was little change in the period of oscillation. This suggests that the mechanisms driving pulsatile myosin behavior during ratcheting were functioning normally despite different levels of cell-ECM adhesion. Therefore, altered ratcheting is unlikely to be the cause of the phenotypes we see (Fig. 3.9. D, H, L).

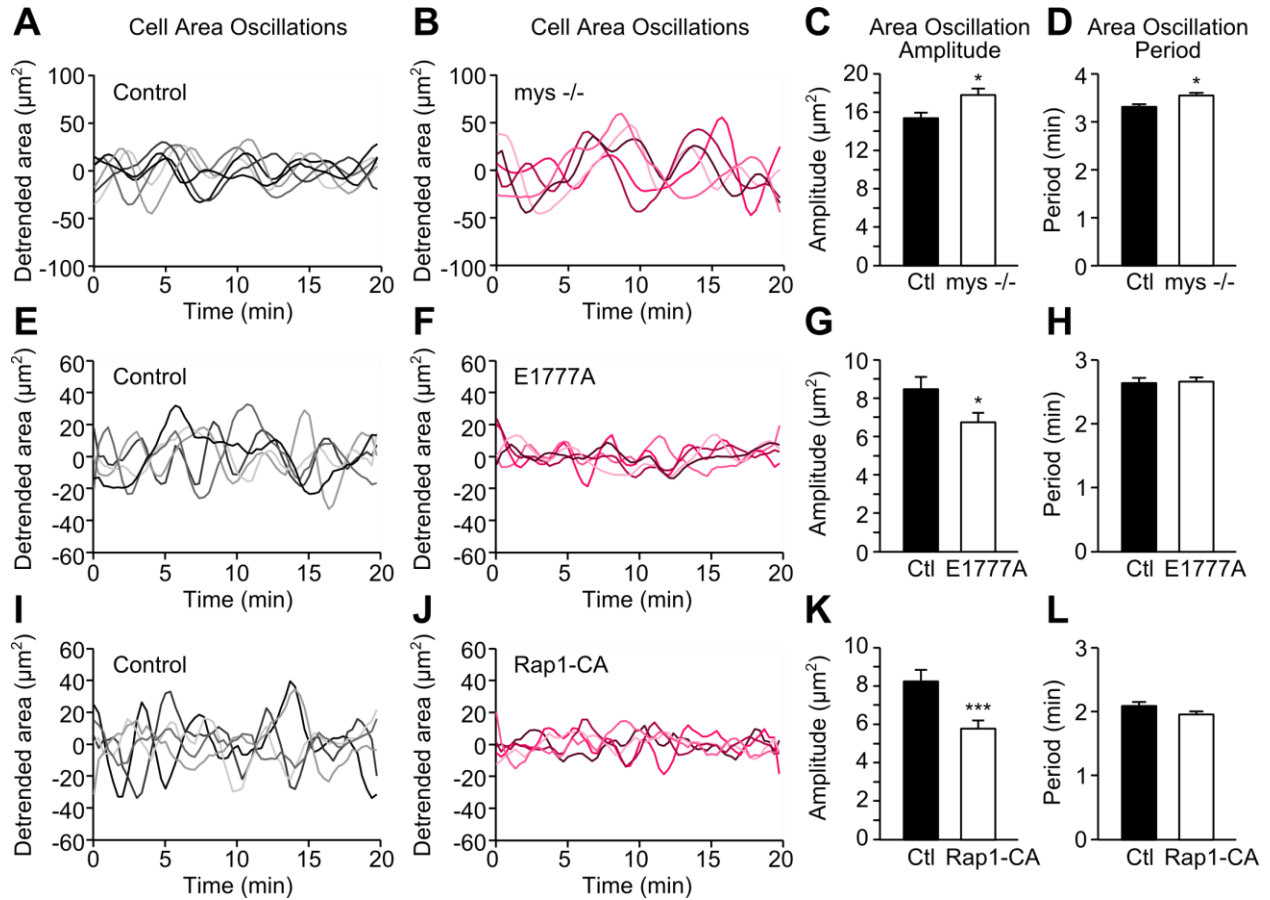


Figure 3.9. Cell-ECM adhesion controls AS cell area oscillations

(A-B, E-F, I-J) Apical area over time of 5 samples AS cells (each line represents a different cell) in *mys*^{-/-} (B), E1777A (F) and Rap1-CA (J) mutants and controls (A, E, I). Areas have been detrended so that their means are at 0. (C, G, K) Amplitude of area oscillations in mutants and controls. (D, H, L) Period of cell area oscillations. Error bars indicate SEM. *** indicates $p < 0.0001$, * $p < 0.05$.

To further investigate the possibility that cell-ECM affects force-generating mechanisms in the AS, we analysed the recoil of junctions over a longer period of time in order to infer tissue biomechanical properties based on different models. We applied two previously used models of recoil: (1) the viscoelastic model, which can be used to infer the ratio of viscosity to stiffness, and (2) the power law model, which can be used to infer fluidity^{90,91}. In integrin mutants, the data was not well fit by either model – instead of junction displacement increasing and then reaching a

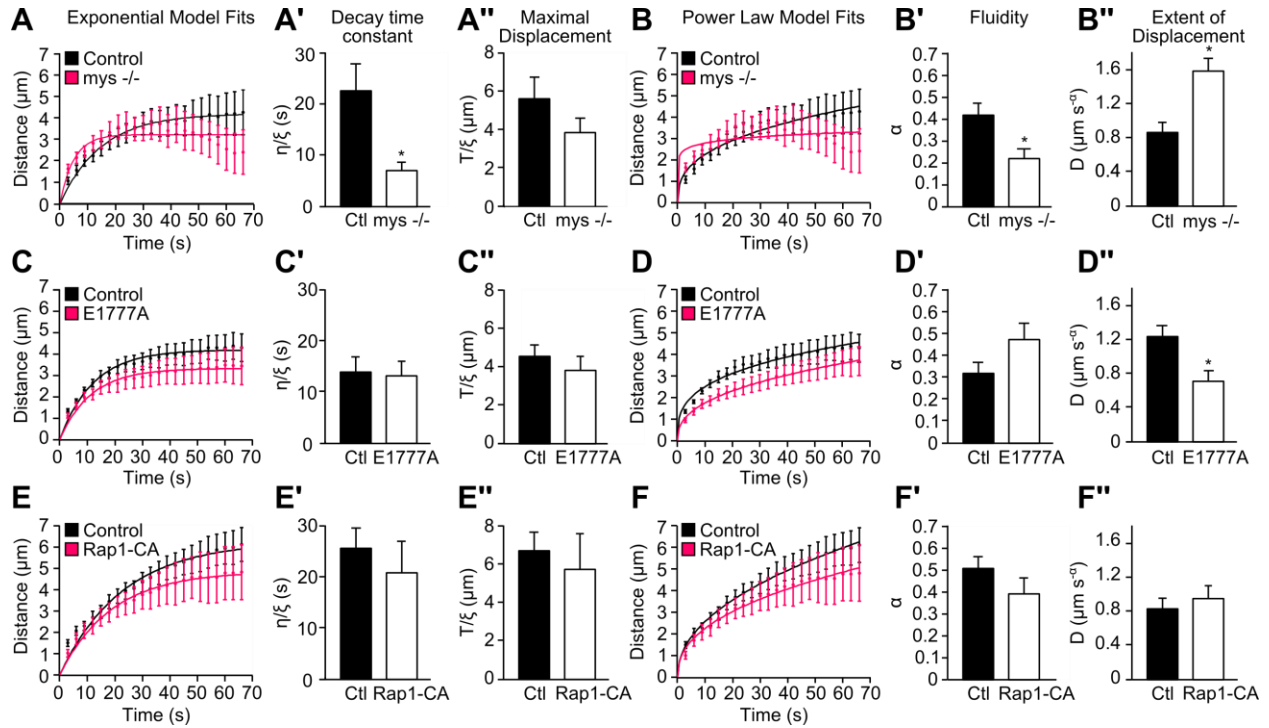


Figure 3.10. Tissue mechanical properties in embryos with altered cell-ECM adhesion

(A-B'') Recoil of cell junctions fit to exponential model (A) and power law model (B) in control and integrin mutant embryos. Points and error bars represent data, line represents fit. (A-A'') Parameter estimates for decay time constant and maximal displacement from exponential model. (B'-B'') Parameter estimates for fluidity and extent of displacement from power law model. (C-D'') Exponential model and power law model fits and parameter estimates in E1777A mutants and controls. (E-F'') Exponential model and power law model fits and parameter estimates in Rap1-CA mutants and controls. Error bars indicate SEM, * indicates $p < 0.05$.

plateau, it typically reached a maximum and then began to decrease, a behaviour not predicted by the models used. We therefore applied the viscoelastic model to only the early parts of the time-lapse, before junction displacement began decreasing, and found that the ratio of viscosity to stiffness is lower in integrin mutants (Fig. 3.10. A-A''). Using the same approach with the power law model, we find that fluidity is lower (more solid-like) and that the extent of displacement is greater than in controls (Fig. 3.10. B-B''). In E1777A and Rap1-CA mutants, we find no changes in the viscoelastic model parameters, similar fluidity, and a decreased extent of displacement in

E1777A (Fig. 3.10. C-F’’). These data suggest that while integrin mutants have altered tissue biomechanical properties, mutants with increased cell-ECM adhesion do not. Since E1777A and Rap1-CA mutants do not appear to have vastly different viscoelastic properties, the tension estimates in these backgrounds are validated. However, the experiments in integrin mutants suggest that viscosity and/or stiffness of AS cells may be affected by removing cell-ECM adhesion, calling into question the tension results in section 3.5.

3.7. Cell-ECM adhesion controls force transmission in the AS.

If we assume that modulating cell-ECM adhesion does not affect tissue biomechanics or actomyosin ratcheting, there must be another mechanism by which integrin-mediated adhesion controls force generation in the AS. We therefore hypothesized that cell-ECM adhesion would control the transmission of tension across the tissue. In order to measure force transmission in the AS, we tracked the movement of second neighbour junctions (2 cell edge segments away from the cut – see Fig. 3.11. A) after laser ablation⁹⁰. If force is readily transmitted, we would expect higher second neighbour recoil velocity, and less decay of recoil effects further away from the cut. Conversely, if force is poorly transmitted, we would expect the opposite: lower second neighbour recoil velocity and more decay of recoil effects. In integrin mutants, which exhibit more cell movement, second neighbour recoil velocity was higher than in controls (Fig. 3.11. A-B). Furthermore, there was less decay of maximum displacement of junctions as a function of distance from the cut than in controls (Fig. 3.11. J-J’). In E1777A and Rap1-CA mutants, where cell mobility is restricted, we saw the opposite effect. Second neighbour recoil velocity was significantly smaller than in controls, and maximal displacement of junctions decayed more quickly with increasing distance from the cut (Fig. 3.11. D-E, G-H, K-L’). Overall, recoil effects following laser ablation are well propagated when cell-ECM adhesion is decreased, but dissipated

when cell-ECM adhesion is increased. These results suggest that cell-ECM adhesion modulates the ability of cells to transmit forces across the AS.

The AS is a highly dynamic tissue – to differentiate normal cell junction movement from recoil effects, we further quantified the movement of junctions more than 3 cell membrane segments away from the cut (>3rd neighbours). In *mys* ^{-/-} mutants, second neighbour recoil was significantly higher than >3rd neighbours, but maximum displacement was not (Fig. 3.11. B-C). The latter finding could be a result of the pattern of junction movement seen in Fig. 3.10. A – instead of increasing in distance consistently as seen in controls, cell junction in *mys* ^{-/-} mutants move back in towards the cut, potentially resulting in less maximum displacement. In E1777A and Rap1-CA mutants, second neighbour recoil was indistinguishable from >3rd neighbour junction movement (Fig. 3.11. E, H), as would be expected in forces are dissipated when cell-ECM adhesion is increased. However, maximum displacement of second neighbours was higher than >3rd neighbours in both E1777A and Rap1-CA mutants (Fig. 3.11. F, I), suggesting that the measured perturbations after recoil are not due solely to background movement. The discrepancy between control results seen in Fig. 3.10. C, F and I, as well as the lower levels of displacement in *mys* ^{-/-} mutants, are likely a result of low laser power – repeating the experiments in *mys* ^{-/-} and controls with increased power may elicit a higher response, bringing junction displacement above background.

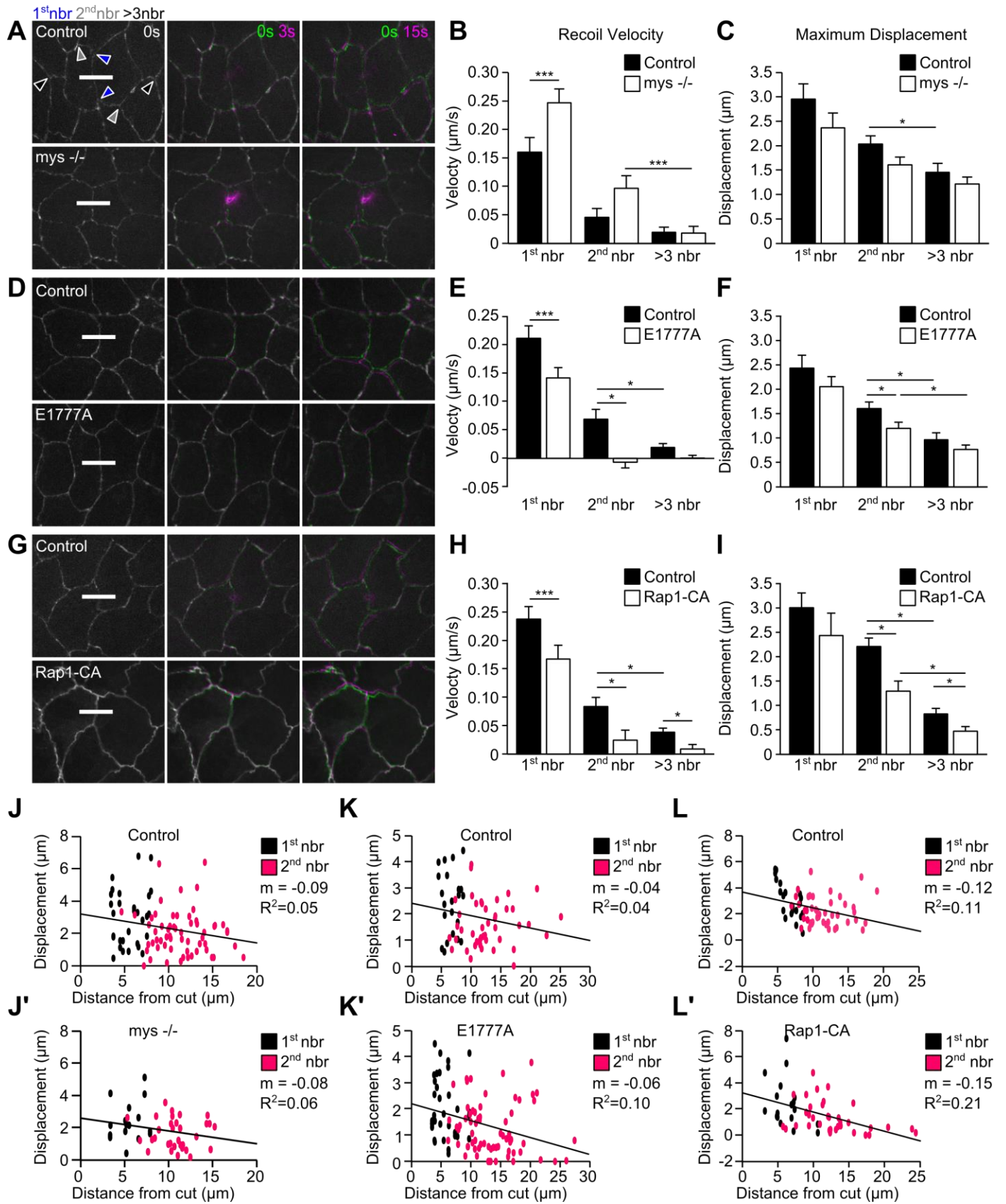


(figure legend on following page)

Figure 3.11. Cell-ECM adhesion controls force transmission in the AS

(A, D, G) AS cells before ablation (left), and at 3 seconds (middle) and 15 seconds (left) after ablation in *mys*^{-/-}, E1777A and Rap1-CA mutant and control embryos. White line indicates location of cut. Examples of 1st (blue), 2nd (grey) and far (≥ 3 , black) neighbour (nbr) junctions are indicated by arrows in (A). (B, E, H) Recoil velocity of 1st, 2nd and $\geq 3^{\text{rd}}$ neighbour junctions in mutants and controls. (C, F, I) Maximum displacement of 1st, 2nd and $\geq 3^{\text{rd}}$ neighbour junctions in mutants and controls. (J-L') Maximum displacement of 1st and 2nd neighbour junctions as a function of distance from the cut in mutants and controls. Slope (m) and R² value of linear fit indicated next to plots. Error bars indicate SEM. *** indicates $p < 0.0001$, * indicates $p < 0.05$.

3.8. Cell-cell and cell-substrate movement correlations in the AS

Cell-ECM adhesion correlates inversely with both cell mobility and transmission of recoil effects – we therefore sought to determine whether the transmission of force was linked to cell movement. To this end, we looked at the correlation of centroid movement in cell pairs in the AS of wild-type, heterozygous (*mys*^{+/-}) and homozygous (*mys*^{-/-}) integrin mutants. We analysed movement along the ML and AP axes of the embryo, and divided cell pairs into first and second neighbours based on the distance between cell centroids. In *mys*^{-/-} mutants, first neighbour cell pairs have a higher correlation coefficient for movement along AP and ML when compared to *mys*^{+/-} and WT (Fig. 3-12. B, E). Furthermore, a greater percentage of both first neighbour and second neighbour pairs were found to move in phase in *mys*^{-/-} mutants than in controls (Fig. 3.12. A, C-D, F-G'). Overall, this data shows that cell movement is highly correlated when cell-ECM adhesion is decreased, which may allow for more efficient transmission of recoil effects after laser ablation. Higher correlation of movement suggests that a single cell's movement or contraction has a greater effect on the neighbouring cells. Therefore, forces exerted by a cell may be more readily transmitted across the tissue when cell-ECM adhesion is reduced.

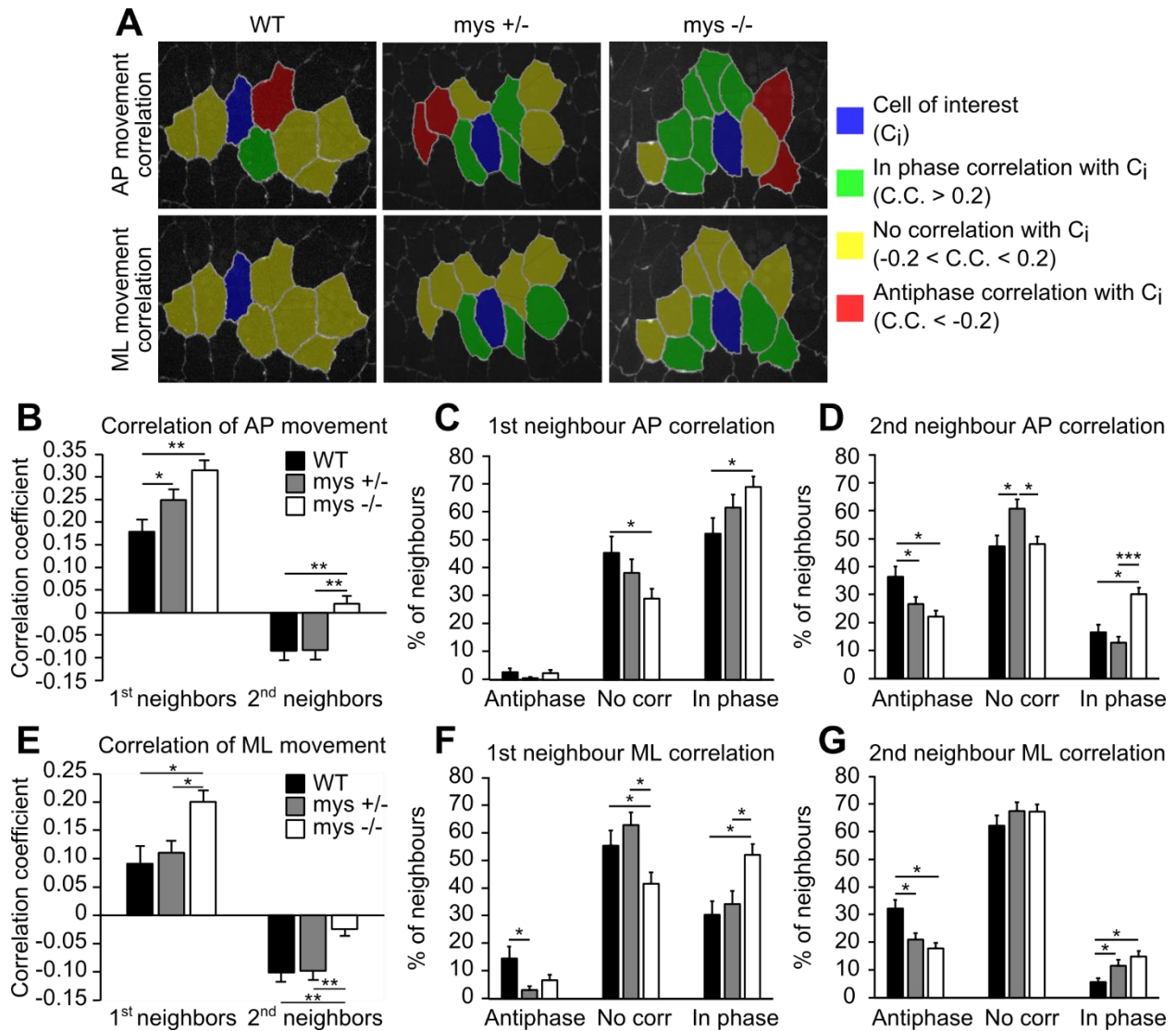


Figure 3.12. Decreased cell-ECM adhesion results in more transmission of cell movement

(A) AS cells in wild-type (left), *mys* heterozygous (*mys +/-*, middle) and homozygous (*mys -/-*, right) mutant embryos colour coded to show AP (upper) and ML (lower) movement correlation with respect to sample cell of interest (C_i , blue). Cells moving in phase with C_i are coloured in green, cells with no correlation with C_i are coloured in yellow, and cells moving antiphase with C_i are coloured in red. (B) Mean correlation coefficient for AP (B) and ML (E) movement of 1st and 2nd neighbour cell pairs. (C-D) % of 1st neighbour (C) and 2nd neighbour (D) cell pairs with in phase, no or antiphase AP movement correlation. (F-G) % of 1st neighbour (F) and 2nd neighbour (G) cell pairs with in phase, no or antiphase ML movement correlation. Error bars indicate SEM. *** indicates $p < 0.0001$, * $p < 0.05$.

In addition to mechanical interactions with their neighbours within the plane of the tissue, cells also exert forces on their substrate – in our case, the ECM and the yolk membrane. To examine cell-substrate interactions, we used fluorescently tagged Basigin (Bsg-GFP), a transmembrane protein found to be highly enriched in extra-embryonic tissues, most notably in the yolk membrane (Fig. 3.13. A-C' and ⁸⁸). By simultaneously tracking the movement of Bsg-GFP intensity using particle image velocimetry (PIV) and the movement of DE-Cad-mTomato labelled cell membranes, we can examine the correlation between cell and substrate movement (Fig. 3.13. D-E). This analysis revealed a positive correlation between cell centroid and Bsg-GFP intensity movement along both ML and AP axes (Fig. 3.13. F-I). Traction force microscopy (TFM) studies in cell culture have shown a negative correlation of cell and substrate^{30,34}. TFM studies employ polyacrylamide gels containing fluorescent beads, and can measure displacement of beads in order to infer traction forces exerted by spreading or migrating cells³⁵. This analysis requires a complete knowledge of the gel's physical properties in order to compute forces exerted by the cell; while we cannot make the same inference in the AS without knowing the physical properties of the ECM and yolk membrane, we can use the movement of Bsg-GFP intensity as an analogue for bead movement in order to infer the direction of force. Unlike TFM studies of migrating cells, we see that Bsg-GFP intensity moves with AS cells, suggesting that these cells may not exert traction on the ECM and yolk membrane, but instead pull their substrate during movement. It seems therefore that while AS cells are mechanically coupled to the substrate, they do not crawl along it as do migrating cells. Whether cell-substrate movement correlations would be affected in increased or decreased cell-ECM adhesion mutants is yet to be determined.

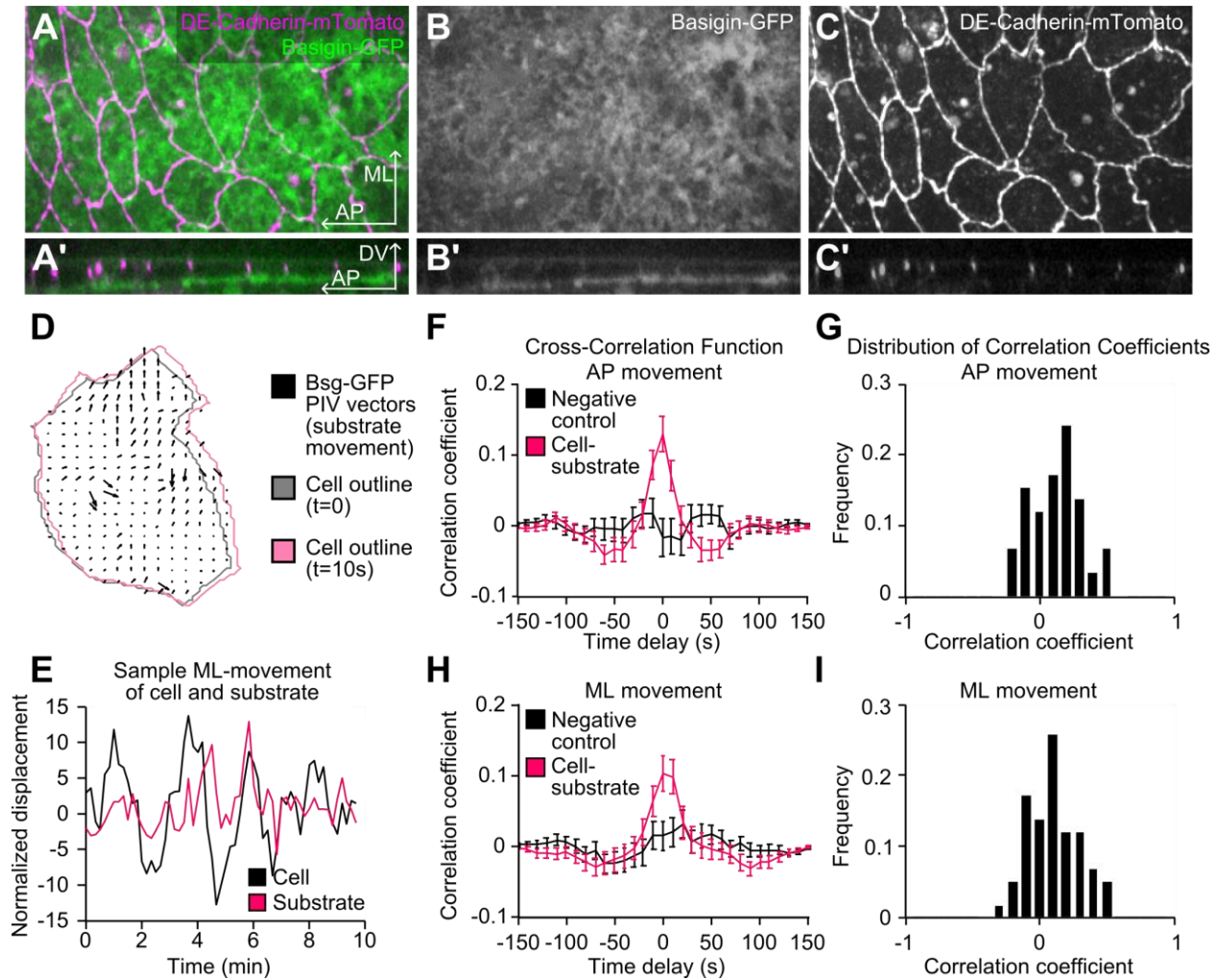


Figure 3.13. AS cell movement correlates with in-plane substrate displacements

(A-C') Sample images of the AS in an embryo expressing Bsg-GFP (green in A-A', alone in B-B') and DE-Cadherin-mTomato (magenta in A-A', alone in C-C'). Dorsal-ventral view reconstructed from z-stacks for merge (A'), Bsg-GFP (B') and DE-Cad-mTomato (C'). AP, ML and DV axes indicated. (D) Sample cell outline at t=0 (grey) and t=30 seconds (pink) with vector field determined by Bsg-GFP PIV (black). (E) Normalized cell centroid ML-displacement (black) and mean ML-displacement of all Bas-GFP PIV vectors within the cell (pink) over the course of 1 time lapse. (F, H) Average cross correlation function of AP (F) and ML (H) movement for all cell-substrate pairs (pink) and negative control (black). (G, I) Distribution of correlation coefficients for AP (G) and ML (I) movement for all cell-substrate pairs. Error bars indicate SEM.

We then extended these analyses to look for substrate deformation along the DV axis of the embryo in order to determine if cells also exerted out-of-plane forces on their substrate, as described in a study which applied 2.5 dimensional TFM to single cells in culture³⁶. We found that changes in AS cell area were highly correlated with displacement along the DV axis of the substrate surface, as defined by the height of maximum Bsg-GFP intensity (Fig. 3.14.). These results indicate that when cells constrict apically, the substrate is pushed downwards (ventrally), and when cell area relaxes, the substrate moves up (dorsally) (Fig. 3.14. E). However, it is still unclear whether substrate deformation along the DV axis is mediated by cell-ECM adhesion or simply a result of yolk and AS cell surface tensions. Nevertheless, these results, along with those presented above, clearly demonstrate that mechanical coupling exists between cells and their substrate within tissues of a developing organism.

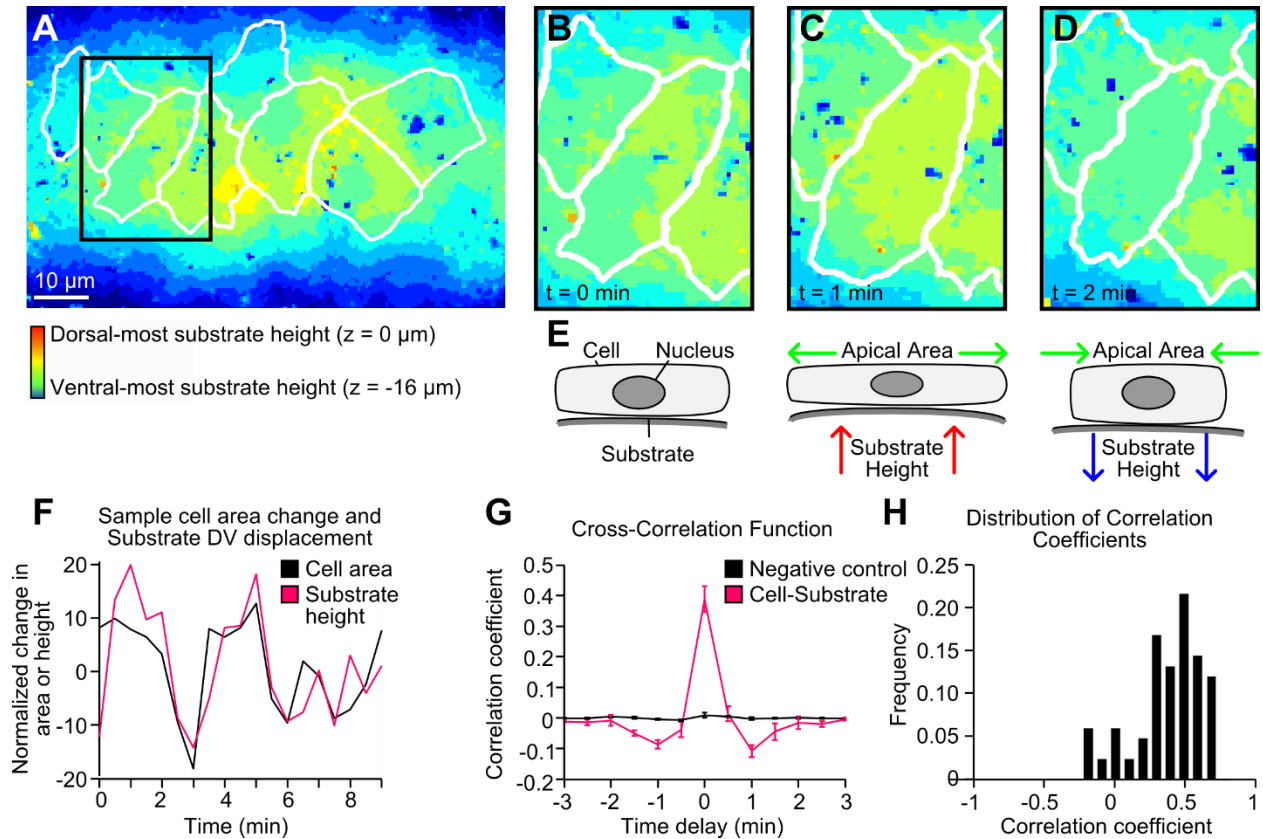


Figure 3.14. Fluctuations in AS cell area are accompanied by changes in substrate height

(A) Heat map of yolk membrane (substrate) height determined by peak Bsg-GFP intensity overlaid with cell outlines (white). Colour bar indicates colour map from lowest points (ventral-most) to highest (dorsal-most). (B-D) Zoomed in views of the region outlined in black in (A) at $t=0$ min (B), $t=1$ min (C) and $t=2$ min (D). (E) Schematic of the side view of AS cells illustrating the coordinated cell area and substrate height changes seen in (B-C). (F) Cell area change and substrate displacement along the DV axis over time for a sample cell. (G) Mean cross-correlation function for all cell-substrate pairs (pink) and negative control (black). (H) Distribution of correlation coefficients of cell area change and substrate DV displacement for all cells. Error bars indicate SEM.

Chapter 4: Discussion

4.1. Overview of findings

Throughout my graduate work, I sought to understand the mechanical role of cell-ECM adhesion during morphogenesis by studying cell and tissue-level behaviours during *Drosophila* DC. To this end, I applied quantitative analyses and biophysical tools to measure the effects of altered cell-ECM adhesion on cell mobility and morphology, and on the generation and transmission of forces in the AS. Through characterization of FALS, I gained sub-cellular insights into regulation of cell-ECM adhesion, and its consequences for the mobility of AS cells. Furthermore, I provide evidence that cell-ECM adhesion-dependent changes in cell mobility can be translated into changes in tissue tension and force propagation. Genetic perturbation of cell-ECM adhesion leads to altered cell movement and impaired transmission of tension in the AS.

For this thesis, I built upon previous work in our lab characterizing FALS – adhesive structures in the AS which share many similarities with FAs. Their growth is dependent on contractility, as revealed by experiments in mutant backgrounds in which rho-dependent actomyosin contraction is affected. Integrins have previously been shown to play a force-sensing role in *Drosophila* myotendinous junctions where integrin turnover is modulated in order to stabilize junctions in response to muscle contraction⁹⁹. We believe that FALS present a second instance in which force-sensing via integrins plays an important role in morphogenesis. Similar adhesive structures have been described during *Drosophila* oogenesis – in this context, they mediate the migration of the follicular epithelium, a critical step in egg chamber elongation^{94,96}. Similarly, we have shown that FALS morphology is linked to cell mobility in the AS.

The movement and oscillations of AS cells during DC are modulated by the amount of cell-ECM adhesion. Moreover, the role of cell-ECM adhesion is of definitive importance to DC,

as evidenced by previously known closure defects^{15,57}, and by the delays and abnormal tissue shape evolution documented in this thesis. Given that AS contraction patterns deviated from control embryos, and that AS cell movement is controlled by mechanosensitive adhesion sites, we concluded that cell-ECM adhesion likely plays an important mechanical role during DC.

To gain further insight into the role of cell movement in this context, we also described patterns of cell mobility amongst individual cells in the AS. Using cell tracking and laser ablation, we found that these patterns correlate with patterns of tension distribution. Force inference approaches and assessment of tissue strain had previously predicted that differences in tension between inner and outer AS cells contribute to the contraction of the AS at mid-DC^{98,100}. Our laser ablation experiments provide direct evidence for this phenomenon and moreover, show that these patterns of tension emerge concomitant with increasingly polarized movement of outer AS cells towards the midline. Differential patterns of tension during multicellular movement have also been described in collective cell migration *in vitro*, where leader cells can transmit forces to cells further back via cell-cell adhesions causing a buildup of tension with increasing distance from the leading edge³¹.

We also quantified spatial differences in cell movement during DC in mutants with altered cell-ECM adhesion, and found patterns that suggested cell-ECM adhesion regulates tissue tension. The observed cell movement phenotypes, as well as our measurements of tissue shape evolution over the course of DC, were consistent with expected outcomes if abnormal contractile forces were arising in the AS. Laser ablation experiments revealed that tissue tension correlates inversely with the amount of cell-ECM adhesion, in line with our predictions regarding tissue contraction. However, there are multiple possible mechanisms by which integrins could be regulating tensile force.

Integrin-mediated adhesion could be controlling tissue biomechanical properties such as viscosity or stiffness, resulting in altered recoil velocity after ablation. To address this, we examined the recoil of junctions after ablation in the context of two models - one that can be used to infer the ratio of viscosity to stiffness, and the other to infer tissue fluidity^{90,91}. While our mutants with increased cell-ECM adhesion showed similar biomechanical properties to controls, integrin null mutants exhibited increased stiffness and fluidity. It is possible that removal of integrins has consequences for the structure and mechanics of actomyosin networks, a distinct possibility given that in single cell culture models, inhibition of focal adhesion formation prevents the bundling of actin into stress fibers¹⁰¹. However, since the integrin null data was not well fit by either model, we cannot come to any definite conclusions about tissue biomechanical properties inferred in this background.

Another possible mechanism by which cell-ECM adhesion could control tissue tension is through disrupting the ratcheting machinery within cells. While we did not test this directly by examining the behaviour of myosin, we looked at the oscillatory dynamics of cells in the background of altered cell-ECM adhesion. This analysis revealed an inverse correlation between cell-ECM adhesion and oscillation amplitude, an expected result in light of our cell movement phenotypes. If the mechanisms driving pulsatile behaviour were affected, we would expect to see changes in the period of oscillation. Given that our cell-ECM adhesion mutants showed very modest and, for the most part, non-significant differences in period, we concluded that these mechanisms were largely unaffected.

Finally, we tested the possibility that cell-ECM adhesion may control how effectively cells can transmit tension across the AS. By studying the propagation of recoil away from the ablation site, we were able to gain insight into force transmission in backgrounds of varied cell-ECM

adhesion. In the case of decreased adhesion, the effects of laser ablation were well transmitted, while increasing adhesion caused dissipation of recoil effects. These findings parallel those of a recent *in vitro* study in epithelial cell clusters, which showed that downregulation of cell-ECM adhesion resulted in more force transmission across cells³⁰. This finding led us to back to our cell movement experiments, where we looked at the relative movement of nearby cells in the AS. We found that when cell-ECM adhesion was decreased, cell movement was more highly correlated – once again indicative of more efficient transmission of force. This phenotype has been predicted using mathematical modelling of a 1 dimensional chain of mechanochemical oscillators, i.e. viscoelastic elements subject to a concentration-dependent contractile element, experiencing friction¹⁰². When friction is reduced to zero, force is conserved across the chain and all of the segments oscillate together¹⁰², similarly to when cell-ECM adhesion is decreased and cell movement is more highly correlated.

Since multicellular clusters exert forces not only on each other but also on their substrate, we tested whether cells in the AS transmit forces to the underlying ECM lining the yolk cell. We found that as AS cells move, they displace the substrate in the same direction as cell motion, unlike cells migrating on TFM gels, which exert traction on the substrate and therefore displace fluorescent beads in the direction opposite to migration. We also found that substrate displacements occurred along the DV axis, and were highly correlated with apical area changes of AS cells. These results suggests that AS cells are mechanically coupled to their environment, and that crosstalk between cell-cell and cell-ECM forces described *in vitro* may play a role in transmitting forces and controlling cell movement during DC. While we have not yet tested the effect of misregulated integrin adhesion on cell-ECM forces, we hypothesize that in integrin null mutants where cell-cell forces are enhanced, movement coupling between AS cells and the

substrate may be lost, as has been observed by downregulating cell-ECM adhesion in epithelial clusters³⁰. Further, we expect that in the case of increased cell-ECM adhesion, cell-cell force transmission and therefore movement coupling would be hindered due to increased force transmission to the ECM, which may manifest as a higher correlation between cell and ECM movement.

Our data is consistent with the mechanical role of integrins demonstrated in studies of collective cell migration and force transmission during morphogenesis. For example, during closure of the mammalian eyelid, integrin-dependent cell intercalation drives collective migration of an epithelial sheet¹⁰³. In zebrafish development, integrin adhesion to the ECM plays a critical role in axis elongation by controlling the mechanics and adhesion of tissue layers⁸⁶. Our findings build upon the conclusions of these prior studies as we have been able to link tissue-level phenotypes to individual cell behaviours as well as to the subcellular cell-ECM adhesion complexes termed here as FALS. Overall, we conclude that integrin-mediated adhesion plays an important role in coordinating the forces which drive DC. Changes in cell mobility and movement patterns appear to be a result of cell-ECM mediated force transmission. Misregulation of cell-ECM adhesion affects AS contractile forces, and consequently, DC is defective or delayed. We believe that our findings reveal an exciting system in which to study the coupling of cell-cell and cell-ECM movement and forces described in *in vitro* cell migration research in the context of a living, developing organism.

4.2. Limitations and proposed future work

4.2.1. Potential confounding factors

While we primarily examined the role of the AS during DC, and we have reason to believe that the effect of cell-ECM mediated force transmission in the AS is important for DC, there are

many parallel processes occurring which could also explain our phenotypes. The advancement of the surrounding epithelia is just as important as the contraction of the AS during DC. Modulating cell-ECM adhesion could affect the way in which these cells migrate dorsally. The epidermis near the dorsal hole adheres via integrins to a layer of ECM on top of the mesoderm and then later the endoderm as tissues rearrange. If these cells are undergoing a form of collective migration during DC, misregulation of cell-ECM adhesion would affect their movement and could explain DC phenotypes. We have partially addressed this in the case of increased cell-ECM adhesion by expressing a constitutively active form of Rap1 in the AS using the tissue-specific driver c381. The phenotype of Rap1-CA was very similar to and perhaps more severe than that of Talin (E1777A), suggesting that increased cell-ECM adhesion in the AS alone is sufficient to disrupt DC. It would also be beneficial to test the effect of decreased cell-ECM adhesion in a tissue-specific manner in order to evaluate the contribution of the AS to integrin mutant phenotypes.

Furthermore, defective zippering has been proposed to explain integrin null mutant phenotypes based on mathematical modelling and the study of tissue shape evolution during closure^{15,27,97}. However, normal filopodia along the leading edge have been described in integrin mutant embryos, so the defect cannot be attributed to the zippering mechanisms themselves⁹⁷. It is also not known how increasing integrin-mediated adhesion would affect zippering, but given that the protrusions which drive this process are based on microtubule dynamics, it is unlikely that they would be affected²⁴.

Another potential confounding factor to consider is the effect of misregulated cell-ECM adhesion on the cytoskeleton and cell-cell adhesions. From cell culture work we know there is a great deal of communication between FAs and the actin cytoskeleton, as well as cross-talk between cell-cell and cell-ECM adhesions^{42,46}. Recent work has also shown that integrin $\beta 1$ is required for

the proper localization of cadherin and thus of cell-cell junction integrity during mammalian vasculature development¹⁰⁴. While our analysis of cell oscillations and recoil experiments suggested that actomyosin pulsatile behaviour was unaffected in mutants with increased cell-ECM adhesion, there were some discrepancies in integrin null mutants to which abnormal force generation in the AS could be attributed. To directly test this, we could track myosin pulses within AS cells in order to identify changes in flow speed or pulse amplitude and period.

In order to determine if increasing or decreasing cell-ECM adhesion affects cell-cell adhesion, we would need to assess whether recruitment levels and localization of cadherin are altered in our mutant backgrounds. Additionally, we could examine the effects of modulating cell-cell adhesion to see if they replicate any of the mutant phenotypes we observed. Cadherin-mediated adhesion has been demonstrated to play a critical role at the leading edge during DC – embryos expressing a dominant negative form of cadherin fail to form supracellular actin cables and exhibit tears between the epidermis and the amnioserosa even in the early stages of closure¹⁰⁵. Furthermore, AS cells showed a minimal decrease in apical area compared to wild-type¹⁰⁵. Given the demonstrated importance of cadherin-mediated adhesion for DC, and the known interactions between cell-cell and cell-ECM adhesions, it is possible that changes in cell-cell adhesion could explain some of our mutant phenotypes. While the defects described thus far are more severe than those observed in this thesis, disrupting cadherin to a lesser degree may allow us to determine how DC proceeds when cell-cell adhesion is modulated.

4.2.2. Apical vs basal cell dynamics

In this thesis, we attempt to examine the effects of basal adhesion on apical cell and tissue behaviours, a 3 dimensional problem. We have made several assumptions throughout this work about how the apical and basal poles of the cell will behave with respect to each other, without a

complete understand of how their changes in morphology and movement are linked. For the most part, studies similar to this one investigating cell morphology and forces during morphogenesis focus on changes at the apical end of the cell^{8,11,12,97,100}. However, analyses incorporating the entire cell volume have revealed dynamic apical-basal shape changes which contribute to morphogenesis^{10,20}. For example, during *Drosophila* ventral furrow formation, cells have been shown to lengthen and reallocate volume from the apical to the basal portion of the cell, taking on a wedge-like shape¹⁰. Additionally, in the context of DC, caspase-dependent volume loss in AS cells has been demonstrated to play a role in tissue contraction. Over the course of closure, AS cells increase in height as they constrict in apical area²⁰, but at the earliest stages of DC, they are very flat. Given that AS cell volume changes occur over long periods of time, and that there is a minimal distance between apical and basal poles of AS cells, it may be safe to assume that changes at the apical end of the cell are easily transmitted to the basal end and vice versa during oscillatory behaviour in early DC. To test this, we could track cell contours in embryos expressing DE-Cad-mTomato as well as TalinGFP, and compare oscillations and movement using both the apical and basal markers. Additionally, the coupling between apical and basal dynamics could be altered if cell-ECM adhesion is manipulated – for example, movement of the basal end of the cell could lag behind apical movement in mutants with increased cell-ECM adhesion. A lag between the movements of each pole of the cell could account for volume reallocation during apical constriction, which in a simplistic side-view slice would resemble a rectangle changing to a parallelogram of equal area. However, our preliminary data examining the DV movement of the yolk membrane suggests that changes in cell height, inferred from changes in yolk membrane height, may be a more likely explanation, in which case apical and basal movement would be

synchronous. This will need to be tested directly with a marker that labels the entire plasma membrane of AS cells.

The same limitation applies to our laser ablation experiments – while we observed a correlation between recoil and cell-ECM adhesion, we do not know with certainty that this is a result of altered force transmission, or rather a result of local resistance to recoil. To test this, we would once again characterize apical and basal behaviour separately. Using two-channel imaging during ablation experiments, we could look for differences in recoil at the apical and basal ends of the cell. If recoil measured by TalinGFP matches that measured by DE-Cadherin-mTomato, it would indicate that observed results are a result of tissue tension, not of shear stresses across the apical-basal axis. However if recoil differs between the two, then we can conclude that the different recoil velocities are the result of varied frictional resistance. It would also be beneficial to perform this experiment with a range of laser powers in order to assess the effects of different cut depths.

4.2.3. Mathematical model of DC

While the mathematical model used in this thesis produced the same effect on cell centroid movement as seen in our experimental data, it was not able to fully recapitulate the mutant phenotypes we see – namely that decreased friction factor resulted in decreased closure time. This could be for a variety of reasons; for example, the model only accurately represents the early stages of closure and excludes cell extrusion and zippering. If our DC phenotypes were due solely to factors other than the AS, this would explain discrepancies between our data and the model. Alternatively, it is possible that the parameter we chose to modulate is not an effective representation of cell-ECM adhesion. The “friction” factor in this model represents tissue viscosity, and has been named as such in similar models. In order to recapitulate our mutant phenotypes, we may have to separate the concepts of tissue viscosity and friction due to cell-ECM

adhesion. This has already been explored in a 1 dimensional model of oscillators in series, where oscillators were subject to viscoelastic forces and additional external friction¹⁰². Interestingly, setting friction to zero in this model produced a result highly reminiscent of our data concerning correlation of cell movement in an integrin null background. Extending a model like Wang et al.'s to include the effects of external friction might prove useful in understanding how external friction due to cell-ECM adhesion would affect contraction of the AS. Another avenue in which to explore the effects of basal activity and apical dynamics would be to extend this mathematical model to 3 dimensions. This would require the results of the experiments proposed in section 4.2.2, and could provide an opportunity to test our proposed models of how cell-ECM adhesion affects force transmission and cell movement. A 3 dimensional model of DC has already been developed by Saias et al. in order to test the effects of cell volume loss on AS constriction²⁰. However this model does not take into account cell oscillations, but simply the evolution of cell height, length and width over the course of closure. Developing a 3 dimensional model in which to study cell pulsing and contraction in the context of a tissue could therefore present a novel contribution to the field.

4.2.4. Cell-substrate interactions

In this thesis we present a novel approach to understanding cell-substrate interactions *in vivo*, by tracking the intensity of a fluorescently tagged transmembrane protein enriched in the yolk membrane, Bsg-GFP. Using this tool, we have attempted to replicate cell culture experiments using TFM³⁵. Our experiments thus far have shown that cells pull laterally on their substrate during movement, and deform it along the DV axis during oscillation cycles. We believe that this method will be a useful tool in understanding how cells interact with their environment under different conditions. For example, we can apply this technique to the mutants described in this thesis to determine if altered cell-ECM adhesion affects cell-substrate movement coupling. However there

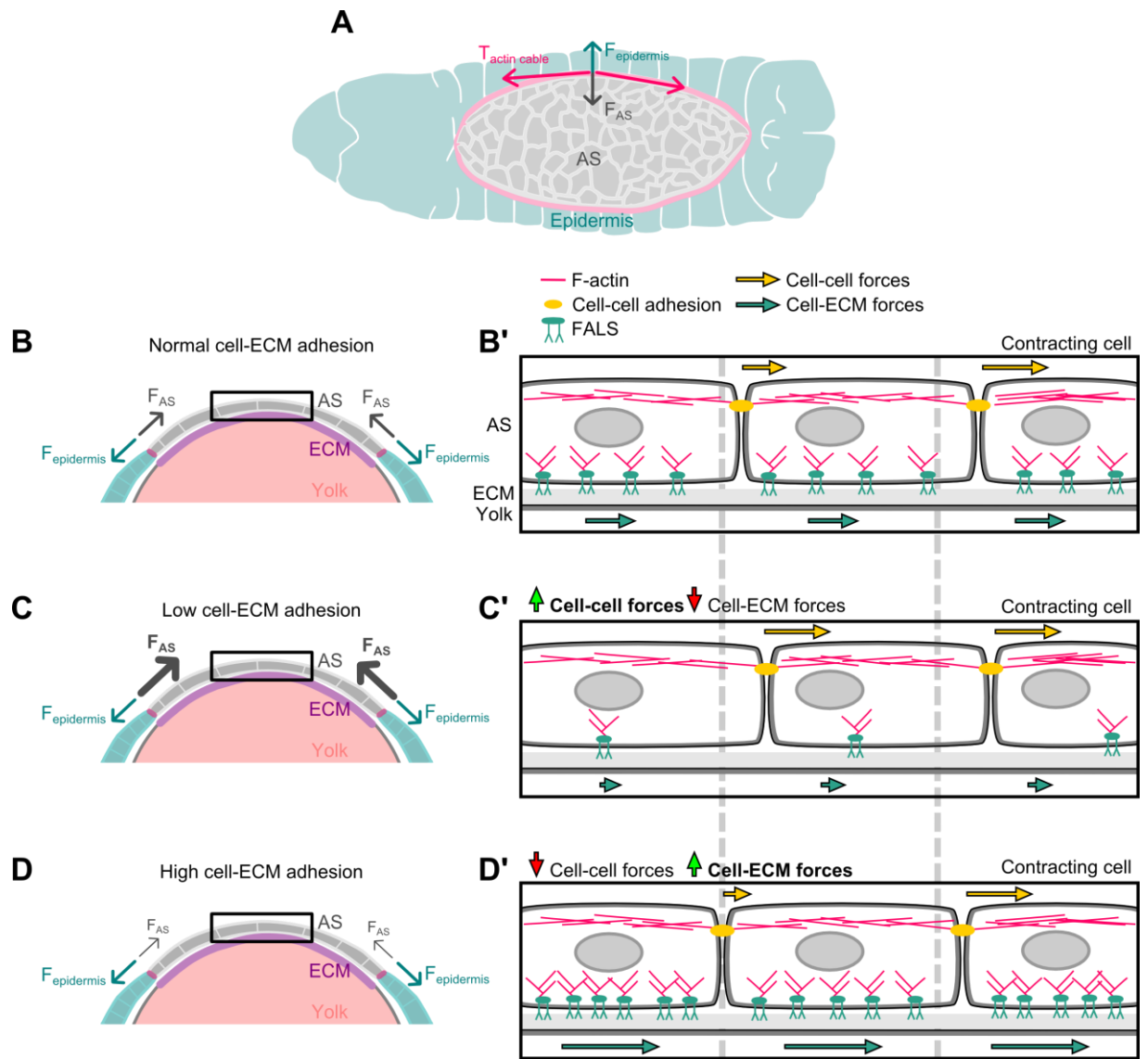
are some assumptions that we make when applying this tool which would have to be validated before further use. Firstly, we must determine with certainty that the Bsg-GFP signal we are tracking is in fact localized to only the yolk membrane. While it has been described as enriched there⁸⁸, it is possible that Bsg-GFP signal from AS cells is also being detected. To address this, we can examine the localization of Bsg-GFP relative to other proteins such as integrin or talin. Additionally, we must confirm that Bsg-GFP intensity movement is a reliable analogue for yolk membrane movement. Is Bsg-GFP stationary or mobile within the yolk membrane? Bsg associates with integrins in mammals¹⁰⁶, and strong genetic interactions between the two have been described in the context of DC in *Drosophila* where they are required for maintaining tissue apposition⁸⁸. Therefore, it is likely that Bsg associates with integrins at the AS-yolk boundary as well. As such, it is possible that Bsg-GFP is anchored by the actin cytoskeleton via integrins, and that it does not undergo significant lateral diffusion, but this could be easily tested by using fluorescence recovery after photobleaching.

Finally, this method could be validated or replaced by developing an alternate way to track yolk membrane movements. One possible way would be to inject fluorescent beads coupled to a molecule which would localize to plasma membranes, such as wheat germ agglutinin¹⁰⁷, into the yolk cell of embryos. Theoretically, this would result in a discrete labelling of the yolk membrane, much like the fluorescent beads embedded in polyacrylamide gels employed in TFM³⁵. While localization and movement relative to the yolk membrane would still have to be determined in order to validate this method, it would likely prove to be a superior method of measuring cell-substrate mechanical interactions. Tracking individual beads is far more reliable than tracking intensity movements of Bsg-GFP, and could allow for higher resolution of substrate displacement. In the Bsg-GFP method, we can examine the overall movement of the substrate relative to a cell,

but to examine differences in substrate movement in different regions beneath cell or at the level of FALS would be very difficult because the technique is imprecise and noisy. Tracking individual beads beneath different parts of a moving cell, or in proximity to FALS, would yield far more detailed information about how AS cells interact mechanically with the yolk membrane.

4.3. Conclusion

Based on the results presented in this thesis we propose the following speculative model (Fig. 4.1.). Cell-ECM adhesion between AS cells and the yolk provides mechanical cell-substrate coupling, and serves to control force transmission during DC. When cell-ECM adhesion is reduced, force transmission to the substrate would theoretically be lessened, while cell-cell forces would be increased (Fig. 4.1. D'). Alternatively if cell-ECM adhesion is increased, forces may be more readily transmitted to the substrate, resulting in decreased cell-cell forces (Fig. 4.1. E'). Force transmission between cells is likely critical for building up tissue tension in the AS that is required for DC. This is supported by the fact that when cell-ECM adhesion is increased, we see decreased force transmission and tension, and misregulated contraction of the AS (Fig. 4.1. E). Conversely, when cell-ECM adhesion is decreased, tissue tension and in-plane force transmission are increased, and AS contraction is mostly unaffected (Fig. 4.1. D). Failure to complete DC in *mys* -/- mutants may not be a result of altered AS-generated forces, but perhaps due to failure of other, peripheral mechanisms, or due to loss of adhesion between the AS and the epidermis. Overall, we propose that the AS is an ideal *in vivo* system within which to understand how cell-cell and cell-ECM forces contribute to morphogenetic movements. Furthermore, we hypothesize that rheostatic control of force transmission through modulation of cell-ECM adhesion may represent a conserved mechanism for the coordination of forces during animal morphogenesis.



4.1. Proposed model for cell-ECM adhesion-mediated force transmission in the AS

(A) Schematic of the dorsal view of an embryo (reproduced with permission from Emily Lostchuck) and diagram of forces involved in DC: F_{AS} , $F_{epidermis}$ and $T_{actin\ cable}$ (defined in Fig. 1.2.)

(B) In the case of normal cell-ECM adhesion, F_{AS} opposes $F_{epidermis}$ to help close the dorsal hole. (B') Zoomed in view of the region in the box in (B) showing side-view schematic of AS cells adhering to ECM above the yolk cell via FALS and to each other via cell-cell adhesion. Cell-ECM forces (teal arrows) are transmitted via FALS, and cell-cell forces (yellow) arrows are transmitted via cell-cell adhesions. Contracting cell (right) will transmit tension to cells to the left, and each cell will transmit forces to the substrate. Cell-ECM forces will cause cell-cell force dissipation with increasing distance from contracting cell. (C-C') In the case of low cell-ECM adhesion, tissue tension is increased resulting in increased F_{AS} , and cell-cell forces will be more readily transmitted (resulting in more movement) due to less opposition by cell-ECM forces. (D-D') In the case of high cell-ECM adhesion, tension and F_{AS} are lower, and cell-cell forces will be quickly dissipated (resulting in less movement) due to increased opposition by cell-ECM forces.

References

- 1 Farge, E. Mechanotransduction in development. *Current topics in developmental biology* **95**, 243-265, doi:10.1016/B978-0-12-385065-2.00008-6 (2011).
- 2 Lecuit, T. & Lenne, P. F. Cell surface mechanics and the control of cell shape, tissue patterns and morphogenesis. *Nature reviews. Molecular cell biology* **8**, 633-644, doi:10.1038/nrm2222 (2007).
- 3 Wozniak, M. A. & Chen, C. S. Mechanotransduction in development: a growing role for contractility. *Nature reviews. Molecular cell biology* **10**, 34-43, doi:10.1038/nrm2592 (2009).
- 4 Lecuit, T., Lenne, P. F. & Munro, E. Force generation, transmission, and integration during cell and tissue morphogenesis. *Annual review of cell and developmental biology* **27**, 157-184, doi:10.1146/annurev-cellbio-100109-104027 (2011).
- 5 Evans, N. D., Oreffo, R. O., Healy, E., Thurner, P. J. & Man, Y. H. Epithelial mechanobiology, skin wound healing, and the stem cell niche. *Journal of the mechanical behavior of biomedical materials* **28**, 397-409, doi:10.1016/j.jmbbm.2013.04.023 (2013).
- 6 Nieto, M. A. Epithelial plasticity: a common theme in embryonic and cancer cells. *Science* **342**, 1234850, doi:10.1126/science.1234850 (2013).
- 7 Mao, Y. *et al.* Differential proliferation rates generate patterns of mechanical tension that orient tissue growth. *The EMBO journal* **32**, 2790-2803, doi:10.1038/emboj.2013.197 (2013).
- 8 Bertet, C., Sulak, L. & Lecuit, T. Myosin-dependent junction remodelling controls planar cell intercalation and axis elongation. *Nature* **429**, 667-671, doi:10.1038/nature02590 (2004).
- 9 Wang, Y. C., Khan, Z., Kaschube, M. & Wieschaus, E. F. Differential positioning of adherens junctions is associated with initiation of epithelial folding. *Nature* **484**, 390-393, doi:10.1038/nature10938 (2012).
- 10 Gelbart, M. A. *et al.* Volume conservation principle involved in cell lengthening and nucleus movement during tissue morphogenesis. *Proceedings of the National Academy of Sciences of the United States of America* **109**, 19298-19303, doi:10.1073/pnas.1205258109 (2012).
- 11 Martin, A. C., Kaschube, M. & Wieschaus, E. F. Pulsed contractions of an actin-myosin network drive apical constriction. *Nature* **457**, 495-499, doi:10.1038/nature07522 (2009).
- 12 Blanchard, G. B., Murugesu, S., Adams, R. J., Martinez-Arias, A. & Gorfinkiel, N. Cytoskeletal dynamics and supracellular organisation of cell shape fluctuations during dorsal closure. *Development* **137**, 2743-2752, doi:10.1242/dev.045872 (2010).
- 13 Wang, Q., Feng, J. J. & Pismen, L. M. A cell-level biomechanical model of *Drosophila* dorsal closure. *Biophysical journal* **103**, 2265-2274, doi:10.1016/j.bpj.2012.09.036 (2012).
- 14 Machado, P. F., Blanchard, G. B., Duque, J. & Gorfinkiel, N. Cytoskeletal turnover and Myosin contractility drive cell autonomous oscillations in a model of *Drosophila* Dorsal Closure. *The European Physical Journal Special Topics* **223**, 1391-1402, doi:10.1140/epjst/e2014-02197-7 (2014).
- 15 Hutson, M. S. *et al.* Forces for morphogenesis investigated with laser microsurgery and quantitative modeling. *Science* **300**, 145-149, doi:10.1126/science.1079552 (2003).

- 16 Kiehart, D. P., Galbraith, C. G., Edwards, K. A., Rickoll, W. L. & Montague, R. A. Multiple forces contribute to cell sheet morphogenesis for dorsal closure in *Drosophila*. *The Journal of cell biology* **149**, 471-490 (2000).
- 17 Jacinto, A., Woolner, S. & Martin, P. Dynamic analysis of dorsal closure in *Drosophila*: from genetics to cell biology. *Developmental cell* **3**, 9-19 (2002).
- 18 Gorfinkiel, N. & Blanchard, G. B. Dynamics of actomyosin contractile activity during epithelial morphogenesis. *Current opinion in cell biology* **23**, 531-539, doi:10.1016/j.ceb.2011.06.002 (2011).
- 19 Toyama, Y., Peralta, X. G., Wells, A. R., Kiehart, D. P. & Edwards, G. S. Apoptotic force and tissue dynamics during *Drosophila* embryogenesis. *Science* **321**, 1683-1686, doi:10.1126/science.1157052 (2008).
- 20 Saias, L. *et al.* Decrease in Cell Volume Generates Contractile Forces Driving Dorsal Closure. *Developmental cell* **33**, 611-621, doi:10.1016/j.devcel.2015.03.016 (2015).
- 21 Jacinto, A. *et al.* Dynamic analysis of actin cable function during *Drosophila* dorsal closure. *Current biology : CB* **12**, 1245-1250 (2002).
- 22 Solon, J., Kaya-Copur, A., Colombelli, J. & Brunner, D. Pulsed forces timed by a ratchet-like mechanism drive directed tissue movement during dorsal closure. *Cell* **137**, 1331-1342, doi:10.1016/j.cell.2009.03.050 (2009).
- 23 Millard, T. H. & Martin, P. Dynamic analysis of filopodial interactions during the zipper phase of *Drosophila* dorsal closure. *Development* **135**, 621-626, doi:10.1242/dev.014001 (2008).
- 24 Jankovics, F. & Brunner, D. Transiently reorganized microtubules are essential for zipper during dorsal closure in *Drosophila melanogaster*. *Developmental cell* **11**, 375-385, doi:10.1016/j.devcel.2006.07.014 (2006).
- 25 Wells, A. R. *et al.* Complete canthi removal reveals that forces from the amnioserosa alone are sufficient to drive dorsal closure in *Drosophila*. *Molecular biology of the cell* **25**, 3552-3568, doi:10.1091/mbc.E14-07-1190 (2014).
- 26 Layton, A. T. *et al.* *Drosophila* morphogenesis: tissue force laws and the modeling of dorsal closure. *HFSP journal* **3**, 441-460, doi:10.2976/1.3266062 (2009).
- 27 Peralta, X. G. *et al.* Upregulation of forces and morphogenic asymmetries in dorsal closure during *Drosophila* development. *Biophysical journal* **92**, 2583-2596, doi:10.1529/biophysj.106.094110 (2007).
- 28 David, D. J., Wang, Q., Feng, J. J. & Harris, T. J. Bazooka inhibits aPKC to limit antagonism of actomyosin networks during amnioserosa apical constriction. *Development* **140**, 4719-4729, doi:10.1242/dev.098491 (2013).
- 29 Schwarz, U. S. & Gardel, M. L. United we stand: integrating the actin cytoskeleton and cell-matrix adhesions in cellular mechanotransduction. *Journal of cell science* **125**, 3051-3060, doi:10.1242/jcs.093716 (2012).
- 30 Ng, M. R., Besser, A., Brugge, J. S. & Danuser, G. Mapping the dynamics of force transduction at cell-cell junctions of epithelial clusters. *eLife* **3**, e03282, doi:10.7554/eLife.03282 (2014).
- 31 Trepap, X., Chen, Z. & Jacobson, K. Cell migration. *Comprehensive Physiology* **2**, 2369-2392, doi:10.1002/cphy.c110012 (2012).
- 32 Parsons, J. T., Horwitz, A. R. & Schwartz, M. A. Cell adhesion: integrating cytoskeletal dynamics and cellular tension. *Nature reviews. Molecular cell biology* **11**, 633-643, doi:10.1038/nrm2957 (2010).

- 33 Geiger, B., Spatz, J. P. & Bershadsky, A. D. Environmental sensing through focal adhesions. *Nature reviews. Molecular cell biology* **10**, 21-33, doi:10.1038/nrm2593 (2009).
- 34 Plotnikov, S. V., Pasapera, A. M., Sabass, B. & Waterman, C. M. Force fluctuations within focal adhesions mediate ECM-rigidity sensing to guide directed cell migration. *Cell* **151**, 1513-1527, doi:10.1016/j.cell.2012.11.034 (2012).
- 35 Plotnikov, S. V., Sabass, B., Schwarz, U. S. & Waterman, C. M. High-resolution traction force microscopy. *Methods in cell biology* **123**, 367-394, doi:10.1016/B978-0-12-420138-5.00020-3 (2014).
- 36 Legant, W. R. *et al.* Multidimensional traction force microscopy reveals out-of-plane rotational moments about focal adhesions. *Proceedings of the National Academy of Sciences of the United States of America* **110**, 881-886, doi:10.1073/pnas.1207997110 (2013).
- 37 Plotnikov, S. V. & Waterman, C. M. Guiding cell migration by tugging. *Current opinion in cell biology* **25**, 619-626, doi:10.1016/j.ceb.2013.06.003 (2013).
- 38 Hall, M. S. *et al.* Toward single cell traction microscopy within 3D collagen matrices. *Experimental cell research* **319**, 2396-2408, doi:10.1016/j.yexcr.2013.06.009 (2013).
- 39 Koch, T. M., Munster, S., Bonakdar, N., Butler, J. P. & Fabry, B. 3D Traction forces in cancer cell invasion. *PloS one* **7**, e33476, doi:10.1371/journal.pone.0033476 (2012).
- 40 Gjorevski, N. & Nelson, C. M. Mapping of mechanical strains and stresses around quiescent engineered three-dimensional epithelial tissues. *Biophysical journal* **103**, 152-162, doi:10.1016/j.bpj.2012.05.048 (2012).
- 41 Campas, O. *et al.* Quantifying cell-generated mechanical forces within living embryonic tissues. *Nature methods* **11**, 183-189, doi:10.1038/nmeth.2761 (2014).
- 42 Maruthamuthu, V., Sabass, B., Schwarz, U. S. & Gardel, M. L. Cell-ECM traction force modulates endogenous tension at cell-cell contacts. *Proceedings of the National Academy of Sciences of the United States of America* **108**, 4708-4713, doi:10.1073/pnas.1011123108 (2011).
- 43 Serra-Picamal, X., Conte, V., Sunyer, R., Munoz, J. J. & Trepate, X. Mapping forces and kinematics during collective cell migration. *Methods in cell biology* **125**, 309-330, doi:10.1016/bs.mcb.2014.11.003 (2015).
- 44 Tambe, D. T. *et al.* Collective cell guidance by cooperative intercellular forces. *Nature materials* **10**, 469-475, doi:10.1038/nmat3025 (2011).
- 45 Maruthamuthu, V., Aratyn-Schaus, Y. & Gardel, M. L. Conserved F-actin dynamics and force transmission at cell adhesions. *Current opinion in cell biology* **22**, 583-588, doi:10.1016/j.ceb.2010.07.010 (2010).
- 46 Liu, Z. *et al.* Mechanical tugging force regulates the size of cell-cell junctions. *Proceedings of the National Academy of Sciences of the United States of America* **107**, 9944-9949, doi:10.1073/pnas.0914547107 (2010).
- 47 Borghi, N., Lowndes, M., Maruthamuthu, V., Gardel, M. L. & Nelson, W. J. Regulation of cell motile behavior by crosstalk between cadherin- and integrin-mediated adhesions. *Proceedings of the National Academy of Sciences of the United States of America* **107**, 13324-13329, doi:10.1073/pnas.1002662107 (2010).
- 48 Friedl, P., Hegerfeldt, Y. & Tusch, M. Collective cell migration in morphogenesis and cancer. *The International journal of developmental biology* **48**, 441-449, doi:10.1387/ijdb.041821 (2004).

- 49 Poujade, M. *et al.* Collective migration of an epithelial monolayer in response to a model wound. *Proceedings of the National Academy of Sciences of the United States of America* **104**, 15988-15993, doi:10.1073/pnas.0705062104 (2007).
- 50 Ladoux, B. *et al.* Force mapping in epithelial cell migration. *Molecular biology of the cell* **15**, 161a-162a (2004).
- 51 Bulgakova, N. A., Klapholz, B. & Brown, N. H. Cell adhesion in *Drosophila*: versatility of cadherin and integrin complexes during development. *Current opinion in cell biology* **24**, 702-712, doi:10.1016/j.ceb.2012.07.006 (2012).
- 52 Hynes, R. O. Integrins: bidirectional, allosteric signaling machines. *Cell* **110**, 673-687 (2002).
- 53 Anthis, N. J. *et al.* The structure of an integrin/talin complex reveals the basis of inside-out signal transduction. *The EMBO journal* **28**, 3623-3632, doi:10.1038/emboj.2009.287 (2009).
- 54 Bokel, C. & Brown, N. H. Integrins in development: moving on, responding to, and sticking to the extracellular matrix. *Developmental cell* **3**, 311-321 (2002).
- 55 Brown, N. H. *et al.* Talin is essential for integrin function in *Drosophila*. *Developmental cell* **3**, 569-579 (2002).
- 56 Nayal, A., Webb, D. J. & Horwitz, A. F. Talin: an emerging focal point of adhesion dynamics. *Current opinion in cell biology* **16**, 94-98, doi:10.1016/j.ceb.2003.11.007 (2004).
- 57 Ellis, S. J. *et al.* Talin autoinhibition is required for morphogenesis. *Current biology : CB* **23**, 1825-1833, doi:10.1016/j.cub.2013.07.054 (2013).
- 58 Ellis, S. J. *et al.* The talin head domain reinforces integrin-mediated adhesion by promoting adhesion complex stability and clustering. *PLoS genetics* **10**, e1004756, doi:10.1371/journal.pgen.1004756 (2014).
- 59 Ellis, S. J., Pines, M., Fairchild, M. J. & Tanentzapf, G. In vivo functional analysis reveals specific roles for the integrin-binding sites of talin. *Journal of cell science* **124**, 1844-1856, doi:10.1242/jcs.083337 (2011).
- 60 Franco-Cea, A. *et al.* Distinct developmental roles for direct and indirect talin-mediated linkage to actin. *Developmental biology* **345**, 64-77, doi:10.1016/j.ydbio.2010.06.027 (2010).
- 61 del Rio, A. *et al.* Stretching single talin rod molecules activates vinculin binding. *Science* **323**, 638-641, doi:10.1126/science.1162912 (2009).
- 62 Goksoy, E. *et al.* Structural basis for the autoinhibition of talin in regulating integrin activation. *Molecular cell* **31**, 124-133, doi:10.1016/j.molcel.2008.06.011 (2008).
- 63 Goult, B. T. *et al.* Structural studies on full-length talin1 reveal a compact auto-inhibited dimer: implications for talin activation. *Journal of structural biology* **184**, 21-32, doi:10.1016/j.jsb.2013.05.014 (2013).
- 64 Dumbauld, D. W. *et al.* How vinculin regulates force transmission. *Proceedings of the National Academy of Sciences of the United States of America* **110**, 9788-9793, doi:10.1073/pnas.1216209110 (2013).
- 65 Goult, B. T. *et al.* RIAM and vinculin binding to talin are mutually exclusive and regulate adhesion assembly and turnover. *The Journal of biological chemistry* **288**, 8238-8249, doi:10.1074/jbc.M112.438119 (2013).

- 66 Song, X. *et al.* A novel membrane-dependent on/off switch mechanism of talin FERM domain at sites of cell adhesion. *Cell research* **22**, 1533-1545, doi:10.1038/cr.2012.97 (2012).
- 67 Lee, H. S., Lim, C. J., Puzon-McLaughlin, W., Shattil, S. J. & Ginsberg, M. H. RIAM activates integrins by linking talin to ras GTPase membrane-targeting sequences. *The Journal of biological chemistry* **284**, 5119-5127, doi:10.1074/jbc.M807117200 (2009).
- 68 Burridge, K. & Chrzanowska-Wodnicka, M. Focal adhesions, contractility, and signaling. *Annual review of cell and developmental biology* **12**, 463-518, doi:10.1146/annurev.cellbio.12.1.463 (1996).
- 69 Chrzanowska-Wodnicka, M. & Burridge, K. Rho-stimulated contractility drives the formation of stress fibers and focal adhesions. *The Journal of cell biology* **133**, 1403-1415 (1996).
- 70 Guilluy, C., Garcia-Mata, R. & Burridge, K. Rho protein crosstalk: another social network? *Trends in cell biology* **21**, 718-726, doi:10.1016/j.tcb.2011.08.002 (2011).
- 71 Riveline, D. *et al.* Focal contacts as mechanosensors: externally applied local mechanical force induces growth of focal contacts by an mDia1-dependent and ROCK-independent mechanism. *The Journal of cell biology* **153**, 1175-1186 (2001).
- 72 Zaidel-Bar, R., Itzkovitz, S., Ma'ayan, A., Iyengar, R. & Geiger, B. Functional atlas of the integrin adhesome. *Nature cell biology* **9**, 858-867, doi:10.1038/ncb0807-858 (2007).
- 73 Wolfenson, H., Lavelin, I. & Geiger, B. Dynamic regulation of the structure and functions of integrin adhesions. *Developmental cell* **24**, 447-458, doi:10.1016/j.devcel.2013.02.012 (2013).
- 74 Yoshigi, M., Hoffman, L. M., Jensen, C. C., Yost, H. J. & Beckerle, M. C. Mechanical force mobilizes zyxin from focal adhesions to actin filaments and regulates cytoskeletal reinforcement. *The Journal of cell biology* **171**, 209-215, doi:10.1083/jcb.200505018 (2005).
- 75 Yao, M. *et al.* Mechanical activation of vinculin binding to talin locks talin in an unfolded conformation. *Scientific reports* **4**, 4610, doi:10.1038/srep04610 (2014).
- 76 Kanchanawong, P. *et al.* Nanoscale architecture of integrin-based cell adhesions. *Nature* **468**, 580-584, doi:10.1038/nature09621 (2010).
- 77 Narasimha, M. & Brown, N. H. Novel functions for integrins in epithelial morphogenesis. *Current biology : CB* **14**, 381-385, doi:10.1016/j.cub.2004.02.033 (2004).
- 78 Pines, M., Fairchild, M. J. & Tanentzapf, G. Distinct regulatory mechanisms control integrin adhesive processes during tissue morphogenesis. *Developmental dynamics : an official publication of the American Association of Anatomists* **240**, 36-51, doi:10.1002/dvdy.22488 (2011).
- 79 Marsden, M. & DeSimone, D. W. Regulation of cell polarity, radial intercalation and epiboly in *Xenopus*: novel roles for integrin and fibronectin. *Development* **128**, 3635-3647 (2001).
- 80 Marsden, M. & DeSimone, D. W. Integrin-ECM interactions regulate cadherin-dependent cell adhesion and are required for convergent extension in *Xenopus*. *Current biology : CB* **13**, 1182-1191 (2003).
- 81 Davidson, L. A., Hoffstrom, B. G., Keller, R. & DeSimone, D. W. Mesendoderm extension and mantle closure in *Xenopus laevis* gastrulation: combined roles for integrin

- alpha(5)beta(1), fibronectin, and tissue geometry. *Developmental biology* **242**, 109-129, doi:10.1006/dbio.2002.0537 (2002).
- 82 Davidson, L. A., Marsden, M., Keller, R. & Desimone, D. W. Integrin alpha5beta1 and fibronectin regulate polarized cell protrusions required for *Xenopus* convergence and extension. *Current biology : CB* **16**, 833-844, doi:10.1016/j.cub.2006.03.038 (2006).
- 83 Bjerke, M. A., Dzamba, B. J., Wang, C. & DeSimone, D. W. FAK is required for tension-dependent organization of collective cell movements in *Xenopus* mesendoderm. *Developmental biology* **394**, 340-356, doi:10.1016/j.ydbio.2014.07.023 (2014).
- 84 Julich, D., Geisler, R., Holley, S. A. & Tubingen Screen, C. Integrinalpha5 and delta/notch signaling have complementary spatiotemporal requirements during zebrafish somitogenesis. *Developmental cell* **8**, 575-586, doi:10.1016/j.devcel.2005.01.016 (2005).
- 85 Lackner, S., Schwendinger-Schreck, J., Julich, D. & Holley, S. A. Segmental assembly of fibronectin matrix requires rap1b and integrin alpha5. *Developmental dynamics : an official publication of the American Association of Anatomists* **242**, 122-131, doi:10.1002/dvdy.23909 (2013).
- 86 Dray, N. *et al.* Cell-fibronectin interactions propel vertebrate trunk elongation via tissue mechanics. *Current biology : CB* **23**, 1335-1341, doi:10.1016/j.cub.2013.05.052 (2013).
- 87 Chou, T. B. & Perrimon, N. The autosomal FLP-DFS technique for generating germline mosaics in *Drosophila melanogaster*. *Genetics* **144**, 1673-1679 (1996).
- 88 Reed, B. H., Wilk, R., Schock, F. & Lipshitz, H. D. Integrin-dependent apposition of *Drosophila* extraembryonic membranes promotes morphogenesis and prevents anoikis. *Current biology : CB* **14**, 372-380, doi:10.1016/j.cub.2004.02.029 (2004).
- 89 Fernandez-Gonzalez, R. & Zallen, J. A. Oscillatory behaviors and hierarchical assembly of contractile structures in intercalating cells. *Physical biology* **8**, 045005 (2011).
- 90 Fischer, S. C. *et al.* Contractile and mechanical properties of epithelia with perturbed actomyosin dynamics. *PloS one* **9**, e95695, doi:10.1371/journal.pone.0095695 (2014).
- 91 Ma, X., Lynch, H. E., Scully, P. C. & Hutson, M. S. Probing embryonic tissue mechanics with laser hole drilling. *Physical biology* **6**, 036004, doi:10.1088/1478-3975/6/3/036004 (2009).
- 92 Levayer, R. & Lecuit, T. Oscillation and polarity of E-cadherin asymmetries control actomyosin flow patterns during morphogenesis. *Developmental cell* **26**, 162-175, doi:10.1016/j.devcel.2013.06.020 (2013).
- 93 Roote, C. E. & Zusman, S. Functions for PS integrins in tissue adhesion, migration, and shape changes during early embryonic development in *Drosophila*. *Developmental biology* **169**, 322-336, doi:10.1006/dbio.1995.1147 (1995).
- 94 Haigo, S. L. & Bilder, D. Global tissue revolutions in a morphogenetic movement controlling elongation. *Science* **331**, 1071-1074, doi:10.1126/science.1199424 (2011).
- 95 Cetera, M. *et al.* Epithelial rotation promotes the global alignment of contractile actin bundles during *Drosophila* egg chamber elongation. *Nature communications* **5**, 5511, doi:10.1038/ncomms6511 (2014).
- 96 Lewellyn, L., Cetera, M. & Horne-Badovinac, S. Misshapen decreases integrin levels to promote epithelial motility and planar polarity in *Drosophila*. *The Journal of cell biology* **200**, 721-729, doi:10.1083/jcb.201209129 (2013).
- 97 Gorfinkiel, N., Blanchard, G. B., Adams, R. J. & Martinez Arias, A. Mechanical control of global cell behaviour during dorsal closure in *Drosophila*. *Development* **136**, 1889-1898, doi:10.1242/dev.030866 (2009).

- 98 Brodland, G. W. *et al.* CellFIT: a cellular force-inference toolkit using curvilinear cell boundaries. *PLoS one* **9**, e99116, doi:10.1371/journal.pone.0099116 (2014).
- 99 Pines, M. *et al.* Mechanical force regulates integrin turnover in *Drosophila* in vivo. *Nature cell biology* **14**, 935-943, doi:10.1038/ncb2555 (2012).
- 100 Blanchard, G. B. *et al.* Tissue tectonics: morphogenetic strain rates, cell shape change and intercalation. *Nature methods* **6**, 458-464, doi:10.1038/nmeth.1327 (2009).
- 101 Burridge, K., Turner, C. E. & Romer, L. H. Tyrosine phosphorylation of paxillin and pp125FAK accompanies cell adhesion to extracellular matrix: a role in cytoskeletal assembly. *The Journal of cell biology* **119**, 893-903 (1992).
- 102 Dierkes, K., Sumi, A., Solon, J. & Salbreux, G. Spontaneous oscillations of elastic contractile materials with turnover. *Physical review letters* **113**, 148102 (2014).
- 103 Heller, E., Kumar, K. V., Grill, S. W. & Fuchs, E. Forces generated by cell intercalation tow epidermal sheets in mammalian tissue morphogenesis. *Developmental cell* **28**, 617-632, doi:10.1016/j.devcel.2014.02.011 (2014).
- 104 Yamamoto, H. *et al.* Integrin beta1 controls VE-cadherin localization and blood vessel stability. *Nature communications* **6**, 6429, doi:10.1038/ncomms7429 (2015).
- 105 Gorfinkiel, N. & Arias, A. M. Requirements for adherens junction components in the interaction between epithelial tissues during dorsal closure in *Drosophila*. *Journal of cell science* **120**, 3289-3298, doi:10.1242/jcs.010850 (2007).
- 106 Berdichevski, F., Chang, S., Bodorova, J. & Hemler, M. E. Generation of monoclonal antibodies to integrin-associated proteins. Evidence that alpha3beta1 complexes with EMMPRIN/basigin/OX47/M6. *The Journal of biological chemistry* **272**, 29174-29180 (1997).
- 107 Lecuit, T. & Wieschaus, E. Polarized insertion of new membrane from a cytoplasmic reservoir during cleavage of the *Drosophila* embryo. *The Journal of cell biology* **150**, 849-860 (2000).